

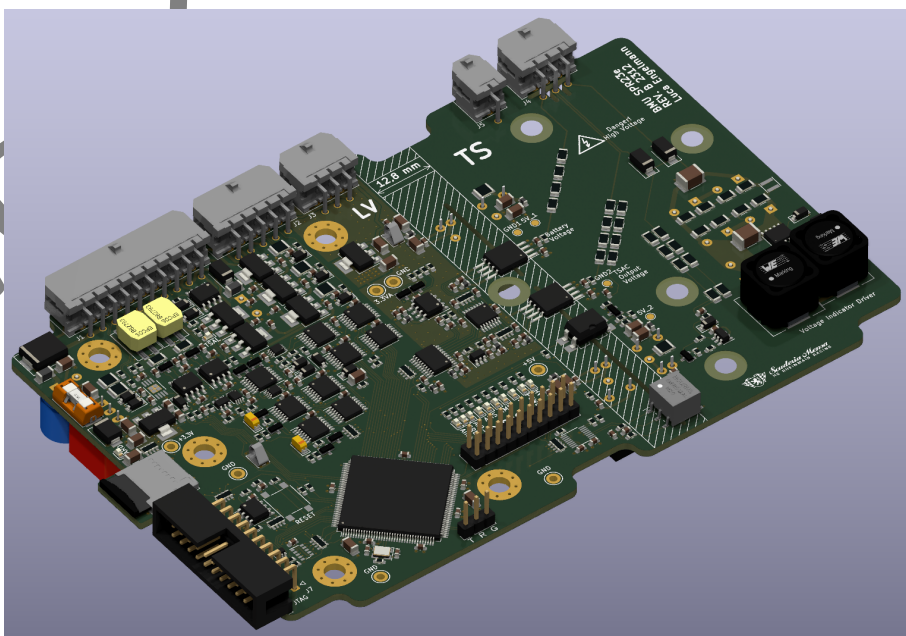
Sauderia Mensa

HS RHEIN MAIN RACING



Design Report

Battery Management System for SPR23e



Department: Electric Drive
Name: Luca Engelmann
Season: 2023/2024



Contents

Glossary	iii
List of Figures	v
List of Tables	vi
1. Introduction	1
1.1. Accumulator	1
1.1.1. System Overview	1
1.2. Requirements	1
1.2.1. General Requirements	1
1.2.2. Rule Requirements	1
1.2.3. Additional Requirements	2
1.2.4. CAN bus interface	3
1.3. SPR21evo BMU	4
1.4. Comparing Legacy and Contemporary Solutions	4
2. BMU Hardware Design	5
2.1. Implementations	5
2.1.1. TSAL	5
2.2. Hardware Block Diagram	5
2.3. Schematic Explanation	5
2.3.1. Power Supply	6
2.3.2. I/O	7
2.3.3. Discharge Control	10
2.3.4. TSAL	11
2.3.5. Shutdown Circuit Control	13
2.3.6. Voltage Indicator driver	14
2.3.7. Isolated TS voltage measurement	16
2.3.8. ADC	17
3. Battery Disconnect Unit	19
3.1. AIR PCB	19
3.2. Current Sensor	21
4. Software Architecture	22
4.1. <Software Modul>	22
5. Test and Validation	23
5.1. Test Setup	23
5.2. TSAL Test	23
6. Potential Improvements	34
7. Bibliography	35
A. Schematics Revision A (Only for reference!)	37



B. Changelog Revision B	50
C. Schematics Revision B	51



Glossary

ADC Analog to Digital Converter

AIR Accumulator Isolation Relay

AMS Accumulator Management System (See BMS)

BDU Battery Disconnect Unit

BMS Battery Management System

BMU Battery Management Unit

BOM Bill Of Material

CAN Controller Area Network

CSV Comma-separated Values

ECU Electronic Control Unit

EMI Electromagnetic Interference

ESD Electrostatic Discharge

FSG Formula Student Germany

HIL Hardware In the Loop

HMI Human Machine Interface

IMD Insulation Monitoring Device

LED Light Emitting Diode

LUT Lookup Table

LVS Low Voltage System

MCU Microcontroller Unit

PCB Printed Circuit Board

RSS root-sum-square

RTC Real Time Clock



SOC State Of Charge

TS Tractive System

TSAC Tractive System Accumulator Container

TSAL Tractive System Active Light

UART Universal Asynchronous Receiver Transmitter



List of Figures

2.1. Top-level BMU schematic.	6
2.2. Schematic of the power supply section.	7
2.3. Schematic of the I/O section.	9
2.4. Schematic of the discharge control section.	10
2.5. Schematic of the TSAL accumulator logic.	11
2.6. Schematic of the shutdown circuit control.	14
2.7. Schematic of the voltage indicator driver.	15
2.8. Schematic of the isolated TS voltage measurement and voltage detection for the TSAL.	16
2.9. Block diagram of the voltage measurement.	18
3.2. Schematic of the AIR PCB	19
3.1. Schematic of the accumulator electronics inside the Battery Disconnect Unit.	20
5.1. TSAL simulation result. Test: No errors.	26
5.2. TSAL HIL result. Test: No errors.	26
5.3. TSAL simulation result. Test: Positive AIR stuck.	27
5.4. TSAL HIL result. Test: Positive AIR stuck.	27
5.5. TSAL simulation result. Test: Pre-charge relay stuck.	28
5.6. TSAL HIL result. Test: Pre-charge relay stuck.	28
5.7. TSAL simulation result. Test: Negative AIR stuck.	29
5.8. TSAL HIL result. Test: Negative AIR stuck.	29
5.9. TSAL simulation result. Test: Voltage detection broken wire.	30
5.10. TSAL HIL result. Test: Voltage detection broken wire.	30
5.11. TSAL simulation result. Test: Positive AIR state detection broken wire.	31
5.12. TSAL HIL result. Test: Positive AIR state detection broken wire.	31
5.13. TSAL simulation result. Test: Pre-charge relay state detection broken wire.	32
5.14. TSAL HIL result. Test: Pre-charge relay state detection broken wire.	32
5.15. TSAL simulation result. Test: Negative AIR state detection broken wire.	33
5.16. TSAL HIL result. Test: Negative AIR state detection broken wire.	33



List of Tables

1.1. Signals of the vehicle CAN interface	4
2.1. Truth table for the plausibility check for each AIR.	11
2.2. Truth table for the TSAC output voltage plausibility check.	12
2.3. Sources of error in each stage of the analog signal chain, type of error, and ability for correction.	17
2.4. Unadjusted and adjusted measurement error of the tractive system voltage measurement using the worst-case and root-sum-square method.	18



1. Introduction

1.1. Accumulator

Kurz auf den Akku eingehen; Zellen, Konfiguration und Rendering.

1.1.1. System Overview

Blockdiagramm mit Stacks, BMS Slave, AIRs und Sicherung, AIR-PCB mit pre-charge und abgesicherte Messabgriffe, Stromsensor, BMU, IMD

1.2. Requirements

1.2.1. General Requirements

The requirements are mostly based on the FSG rule set for 2023 [1]. Some general requirements for the vehicle integration apply also. These include

- Power supply from the low-voltage system (LVS) in a range from 18 V to 25 V, which is the unregulated voltage from the low-voltage accumulator.
- One CAN bus with a bitrate of 1 Mbit/s for the communication with the Vehicle Control Unit.
- One IsoSPI [2] interface for the communication with the BMS slaves on the accumulator stacks.
- Isolated voltage measurement for the accumulator and TSAC output voltage with an accuracy better than 1 % of the full measuring range.
- Isolated current measurement with a resolution better than ± 140 A, which is two times the fuse rating to allow for any short current peaks, and an accuracy better than 1 % of the full measuring range.
- A driver circuit for the voltage indicator must be included on the BMU PCB
- The TSAL accumulator logic must be implemented on the BMU PCB

1.2.2. Rule Requirements

Since the BMU contains many different parts required by the rules, all of the following rules have to be fulfilled. For the TSAL logic in the accumulator these rules apply:

- EV 4.10.3 [p. 85][1] *The TSAL itself must have a green light, continuously on, active if and only if the LVS is active and ALL of the following conditions are true:*
 - *All AIRs are opened.*



- *The pre-charge relay, see EV 5.7.2, is opened.*
- *The voltage at the vehicle side of the AIRs inside the TSAC does not exceed 60 V DC or 50 V AC RMS.*
- EV 4.10.4 [p. 85][1] *The mentioned voltage detection must be performed inside the respective TS enclosure.*
- EV 4.10.5 [p. 85][1] *The mentioned states of the relays (opened/closed) are the actual mechanical states. The mechanical state can differ from the intentional state, i.e. if a relay is stuck. Any circuitry detecting the mechanical state must meet EV 5.6.2.*
- EV 4.10.6 [p. 85][1] *The voltage detection circuit of the red light and the relay state and voltage detection circuit of the green light must be independent. Any plausibility check between both lights is not allowed. A TSAL state with both lights simultaneously active might occur and must not be prevented.*
- EV 4.10.9 [p. 85][1] *The TSAL and all needed circuitry must be hard-wired electronics. Software control is not permitted.*
- EV 4.10.10 [p. 85][1] *A green indicator light in the cockpit that is easily visible even in bright sunlight and clearly marked with “TS off” must light up if TSAL green light is on, see EV 4.10.3.*
- EV 4.10.11 [p. 86][1] *Signals influencing the TSAL and the indicator according to EV 4.10.10 are SCS, see T 11.9. The individual safe state of each of the TSAL lights is off. The TSAL has an active indication of the absence of failures (continuous green illumination) and thus the red light must not be illuminated for a visible check, see T 11.9.5.*
- EV 4.10.13 [p. 86][1] *The TSAL’s green light relay state detection circuit, see EV 4.10.3, does not need to detect an open circuit, as required by T 11.9, when the intentional state of the used (auxiliary) contact is opened. A plausibility check against the intentional relay state must be implemented in a way that the TSAL’s green light stays off after the open circuit is detectable.*
- EV 4.10.14 [p. 86][1] *The TSAL’s green light voltage detection circuit, see EV 4.10.3, does not need to detect an open circuit, as required by T 11.9, when no voltage is present. A plausibility check against the intentional relay states must be implemented in a way that the TSAL’s green light stays off after the open circuit of the accumulator voltage detection circuit is detectable.*
- EV 4.10.14 [p. 86][1] *The latching required by EV 4.10.13 and EV 4.10.14 must not be triggered during normal operation conditions and must only be reset by power cycling the LVS.*

1.2.3. Additional Requirements

Some additional features shall be included on the BMU, which are not necessary to be rule compliant but will help debugging the BMU. These features include:

- Second CAN bus dedicated for diagnosis and remote calibration
- Real Time Clock (RTC) for accurate timestamps
- Logging to an SD card with an interval of 100 ms and timestamps with all necessary signals
- Logfile download via CAN, since the SD card will be buried inside the (sealed) accumulator



-
- UART interface for additional debugging
 - State of Charge (SOC) estimation using a coulomb counter with LUT support
 - Hardware EEPROM for calibration and SOC data
 - The BMU must control the AIRs depending on the requested TS state and always perform a pre-charge sequence
 - A signal that controls the discharge circuit in the inverter housing must be provided by the BMU
 - Status LEDs and debug pins shall be provided on the BMU PCB for easy debugging
 - Test points for important signals shall be provided on the PCB
 - The interface shall use Molex Micro-Fit connectors, since they are used elsewhere in the vehicle and are rated for 600 V

1.2.4. CAN bus interface

The vehicle CAN bus shall only have the minimum amount of data required to minimize the bus load. The whole data, as in the 2022 BMU, is not required since the BMU contains a dedicated logger only for the BMS data. Some actions have to be taken to synchronize the vehicle CAN logger and the BMU logger. This will be done by using the local time of the BMU as Unix timestamp, which is sent on the CAN bus. With the time of the logger, both data sources can be synchronized. Notice, that both RTCs have to be accurately set for this to work. The minimum interface must include the in Table 1.1 listed signals. The listed signals are exchanged with other control units, listed in the ECU column.



Table 1.1.: Signals of the vehicle CAN interface

Name	Description	Direction	ECU	Comment
Battery voltage	Measured battery voltage	Send	VCU	
Battery voltage valid	Validity of battery voltage	Send	VCU	
DC Link voltage	Measured DC Link voltage	Send	VCU	At TSAC output
DC Link voltage valid	Validity of DC Link voltage	Send	VCU	
Battery current	Measured battery current	Send	VCU	
Battery current valid	Validity of battery current	Send	VCU	
Battery power	Calculated instantaneous power	Send	VCU	
Battery power valid	Validity of instantaneous power	Send	VCU	
SOC	State of charge	Send	VCU	Minimum value
SOC valid	Validity of state of charge	Send	VCU	
Min temp	Minimum cell temperature	Send	VCU	
Max temp	Maximum cell temperature	Send	VCU	
Avg temp	Average cell temperature	Send	VCU	
Temperature valid	Validity of temperatures	Send	VCU	
Min cell voltage	Minimum cell voltage	Send	VCU	
Max cell voltage	Maximum cell voltage	Send	VCU	
Avg cell voltage	Average cell voltage	Send	VCU	
Cell voltage valid	Validity of cell voltages	Send	VCU	
Isolation resistance	Isolation resistance reported by IMD	Send	HMI	optional
Isolation resistance valid	Validity of isolation resistance	Send	HMI	optional
TS state	State of the TS state machine	Send	VCU	
Error code	Reason for the TS error	Send	HMI	bit-coded
Contactor state	State of each contactor	Send	HMI	
Timestamp	Unix timestamp	Send	Logger	Data correlation
Reset reason	Last reset reason	Send	all	Only on startup
Permissible discharge (cont)	Continuous allowed discharge	Send	VCU	
Permissible discharge (peak)	Peak allowed discharge	Send	VCU	Fuse I^2t limit
Permissible charge (cont)	Continuous allowed regen. braking	Send	VCU	
Permissible charge (peak)	Peak allowed regen. braking	Send	VCU	Cell limit
TS request	Activate tractive system	Receive	VCU	

1.3. SPR21evo BMU

Kurz auf 21er BMU eingehen, Bild der Platine und Beschreibung der Key Features.

1.4. Comparing Legacy and Contemporary Solutions

Was kann die alte BMU anders als die neue? Welche Features kamen hinzu? Welche sind entfernt worden?
Was ist der Ausblick auf Software-Seite? Logging auf SD-Karte, EEPROM, 2 CAN-Busse

Auch auf AIR-PCB und Stromsensor eingehen



2. BMU Hardware Design

2.1. Implementations

2.1.1. TSAL

The TSAL logic will be implemented in the following way:

- The actual states of the relays will be monitored using auxiliary contacts in the relays. They are mechanically linked to the main contacts as explained in the application note [3, p. 2]: “*The auxiliary contact actuating method will indicate the true position of the main contacts. The auxiliary contact actuation is directly coupled to the main contact moving bridge, and will not indicate “open” unless both contact gaps of the double-make, Form X contact are fully disconnected.*”
- The plausibility check to fulfill EV 4.10.5 is done against the intentional state indicated by the BMU. The following possible states can trigger the latch:
 - The intentional state is active, the actual state reports inactive: A line break in the state detection is to be assumed.
 - The intentional state is inactive, the actual state reports active: The relay is most probably stuck

Due to its mechanical construction, the relay takes 25 ms to switch from the opened to the closed position and 10 ms for the reverse [4, p. 2]. In these time periods, the relay states are implausible and must not trigger the latch, as EV 4.10.14 indicates.

- Likewise, a line break in the voltage detection circuitry is detected using a plausibility check against the relay states. If the relays are closed and the voltage detection circuitry detects no voltage, a fault in the detection circuitry is to be assumed and must lead to the latched deactivation of the green light.
- Since the TSAL accumulator logic is located on the BMU PCB and all TS components needed to perform the checks are located inside the TSAC, EV 4.10.4 is fulfilled.
- The circuit will be build with logic gates without any software control. Therefore, EV 4.10.9 is fulfilled as well. The final circuit is discussed in full detail in section 2.3.4.

2.2. Hardware Block Diagram

Blockdiagramm der BMU Hardware

2.3. Schematic Explanation

The schematic is rather complex and would not fit on one page. It is divided into 11 logical modules, which are connected on the top-level schematic seen in Figure 2.1. Each module will be discussed in the



following subsections. The full schematic is available in Appendix C.

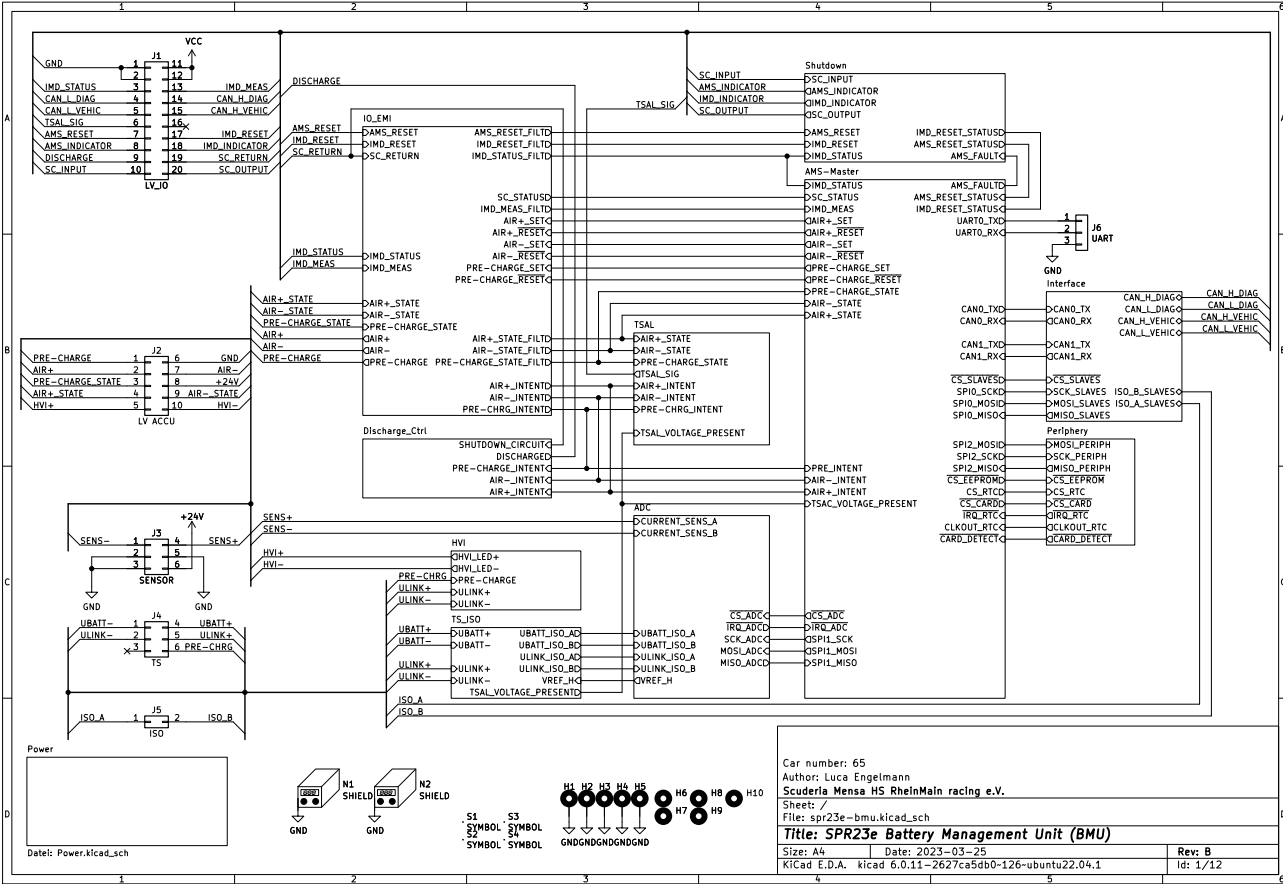


Figure 2.1.: Top-level BMU schematic.

2.3.1. Power Supply

The power supply schematic provides input protection and all necessary power rails for the BMU. The schematic for the power supply section is shown in Figure 2.2. At the input, L1, C77, and C78 form a low-pass filter to filter out any high-frequency noise, which might be on the low-voltage system. D16 is used in conjunction with F1 to protect the BMU against over-voltages. D15 not only protects the BMU from reverse-polarity, but it also isolates the BMU supply from the low-voltage system. A high-current spike will not drain C78, leading to a stable power supply of the BMU in case of voltage dips caused by switching of the cooling fans or pumps. The 18V to 25V provided by the LVS is stepped-down to 5V using an integrated DC to DC converter. Two low-dropout regulators U25 and U26 generate the main 3.3V digital voltage rail used by the microcontroller and the other digital circuits and a secondary 3.3V voltage rail used by the analog circuits. The use of two independent regulators for analog and digital circuits prevents noise coupling from the digital to the analog circuit. A power LED signalizes that the BMU is powered. Test points for all voltage rails are provided for easy measurement on the PCB.

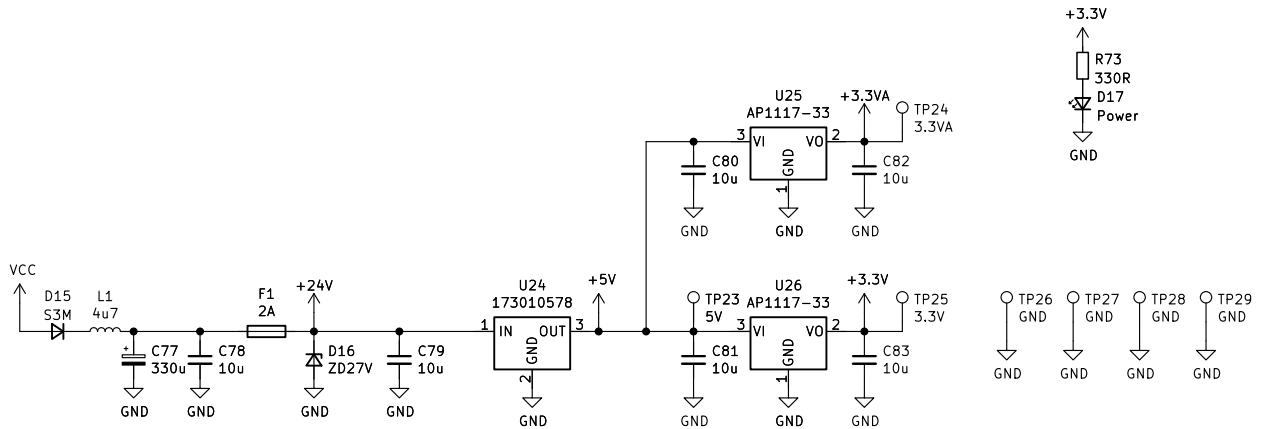


Figure 2.2.: Schematic of the power supply section.

2.3.2. I/O

This section of the schematic conditions the input signals for the BMU logic and drives the AIRs. It can be seen in Figure 2.3. Since the digital section operates at 3.3 V and the signals outside the BMU operate at LVS levels, zener diodes are used to limit the voltages. Each signal has a pull-down resistor to ensure stable logic levels in case of unconnected inputs. The 2.2 k Ω resistors at the inputs for the state detection of each relay ensure the minimum wetting current needed for the LEV100 relays: "*Minimum Aux Contact Load 10mA/12Vdc*" [4, p. 3]. Likewise, the pull-down resistors R77 and R78 for the IMD are the recommended values from the datasheet [5, p. 5]. Note that these resistors have to dissipate some power at the maximum voltage of the LVS: $P_{d,pull-down} = \frac{(25\text{ V})^2}{2.2\text{ k}\Omega} = 0.28\text{ W}$. Therefore, resistors in a 1210 package are used, since they are rated for 0.5 W of power [6]. The capacitors form in combination with the zener diode dropper resistors a low-pass filter used to filter out any noise, which might be picked up by the signal wires. The status of the shutdown circuit is also evaluated by the BMU. The same input protection circuit is used to measure the voltage of it. The relays are directly supplied from the shutdown circuit. L2 and C96 form low-pass filter, which limits the current spike caused by the switching of the relays. D18 is important to separate the high-current path from the detection path. Imagine that the AIRs are not energized and the shutdown circuit is active. Now, one emergency button is pressed. The shutdown circuit is turned off but C96 is still charged. Without D18, it would lead to a false reading of the SC_STATUS signal until the capacitor is discharged. With D18, C96 is blocked from holding up the voltage at the SC_RETURN node in this scenario. This ensures, that the microcontroller and the latches U28A, U28B, and U29A detect a power-loss in the shutdown circuit without any noticeably delay.

The AIRs are controlled by ITS4200 high-side switches [7], which are supplied by the shutdown circuit. This is required by EV 6.1.1 [1]. U30 is used as level shifters to drive the high-side switches. This step is needed, since the ITS4200 is advertised with a "CMOS compatible input" [7, p. 2] and has an input voltage turn-on threshold of 3.0 V [7, Table 4]. Its input is driven with 5 V instead of 3.3 V to avoid potential problems. The inputs of the 74HCT logic series recognize a logical high signal at and above 2.0 V. The ITS4200 is internally protected against short-circuits and voltage backfeed, making it an ideal output driver for the BMU. The relays are not directly controlled by the BMU. Instead, flip-flops isolate the control from the microcontroller to the outputs. The MCU can set and clear the flip-flops. Additionally, the flip-flops can be cleared by the shutdown circuit signal. This has the advantage that the relays are not only de-energized by the loss of power but also the turn-on request is cleared in hardware. In the BMU for the SPR21e, this was solely done in software. Now imagine that the flip-flops were omitted and the microcontroller crashes as soon as the AIRs are energized. If the emergency switch is pushed, the AIRs will de-energize. However,



since the crashed microcontroller still requests the positive and negative AIRs to be energized, re-activation of the emergency switch results in an uncontrolled re-activation of the tractive system without pre-charging. Due to the large current spike, both the positive and negative AIR will be most likely stuck after this event. This has happened in the early testing phase of the SPR21e. With the hardware flip-flops, it doesn't matter if the microcontroller crashes while the AIRs are energized. The flip-flops will only react on the rising-edge of the SET-signals and will be cleared, as soon as the shutdown circuit opens. The intentional states of the relays are taken from the outputs of the flip-flops. Notice that the flip-flops are reset-dominant, meaning that they cannot be set if the clear input is set to a logical zero.

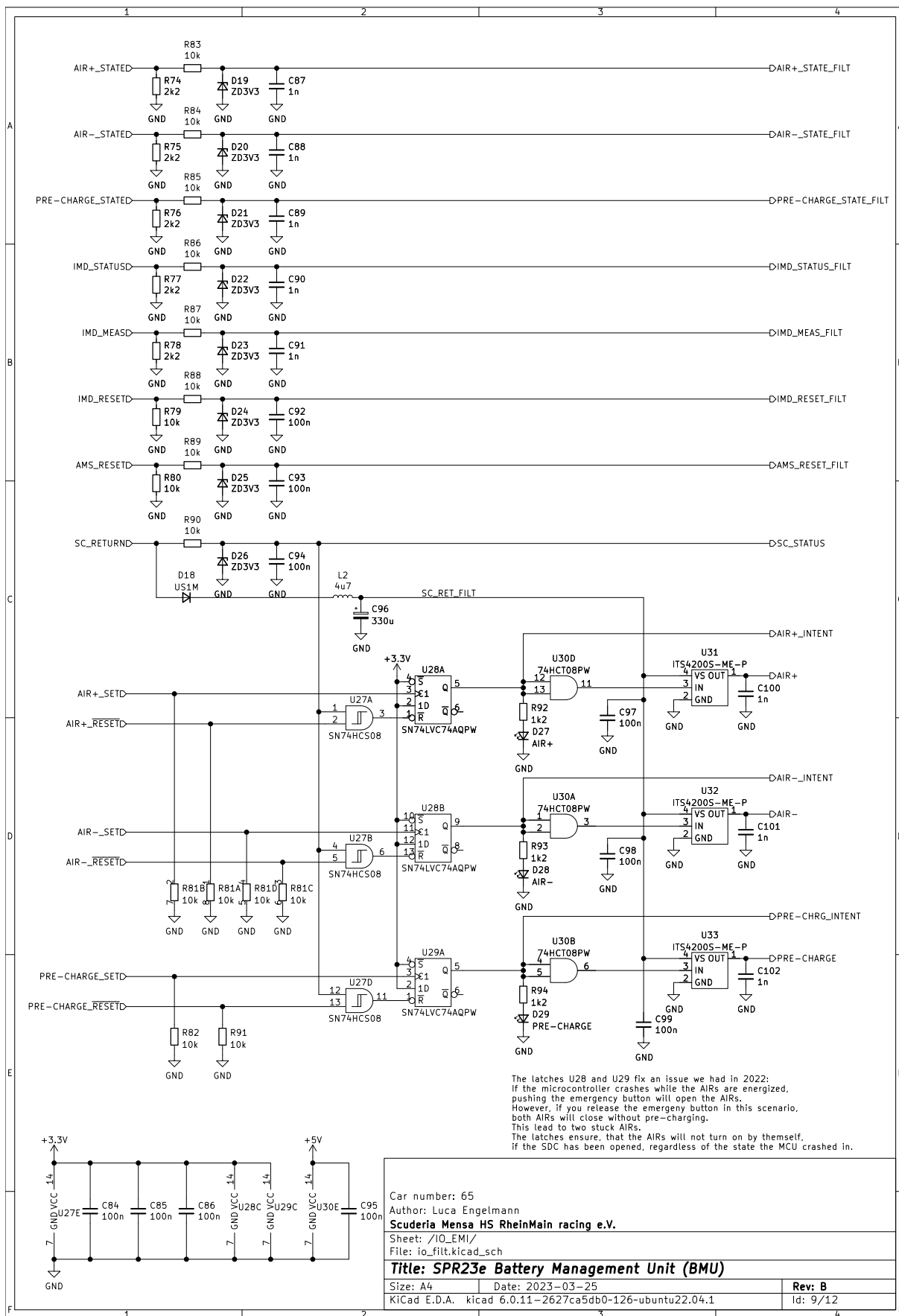


Figure 2.3.: Schematic of the I/O section.



2.3.3. Discharge Control

The discharge circuit is located in the inverter and discharges the DC-Link capacitors within 2 s. Without this circuit, it would take about 30 m for the DC-Link voltage to fall below 60 V. EV 6.1.5 requires the DC-Link voltage to fall within five seconds [1, p. 92]. The discharge circuit is normally active and controlled by the shutdown circuit, as required by EV 4.9.2 [1, p. 84]. If it would be controlled by the shutdown circuit only, it would be de-activated as soon as the shutdown circuit is closed. To add some extra safety, in this design the discharge circuit is controlled by the shutdown circuit and the intentional state of the relays. This ensures, that the discharge circuit is only deactivated if the activation of the tractive system is requested. To ensure that the discharge circuit remains active if the relays are stuck, only the intentional states are used. The discharge is designed to constantly handle the voltage in this scenario, as required by EV 4.9.1 [1, p. 84]. The schematic is shown in Figure 2.4.

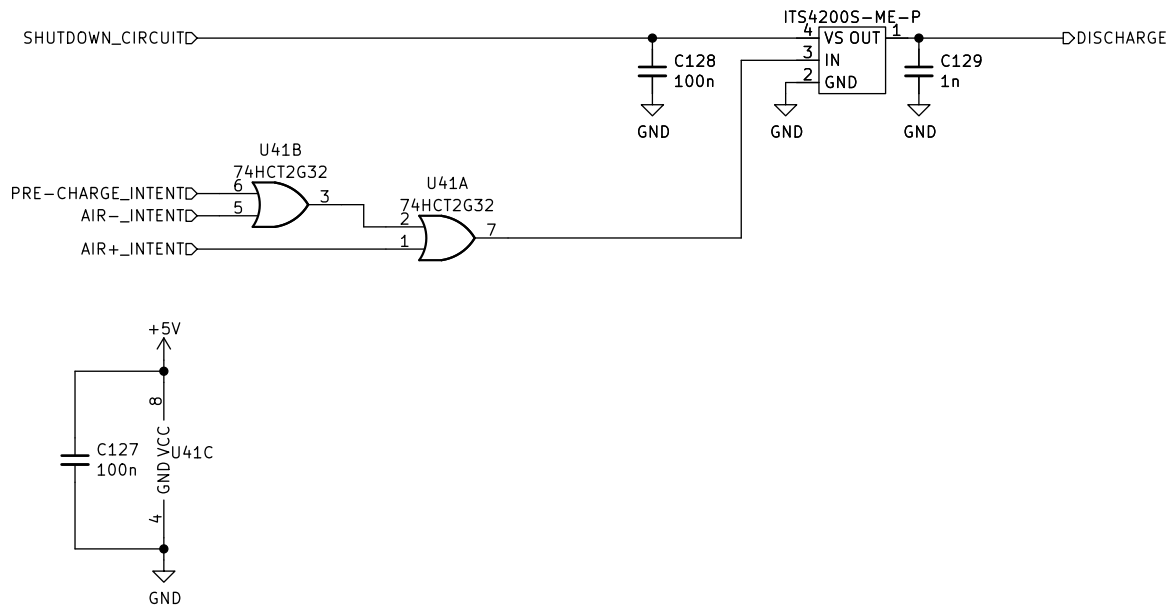


Figure 2.4.: Schematic of the discharge control section.



2.3.4. TSAL

The TSAL schematic can be divided into three logical sections. The top section checks the three AIRs for plausible states. The second section checks the TS detection circuit for plausibility. The third section controls the green light and contains the required latch. Figure 2.5 shows the schematic of the TSAL logic.

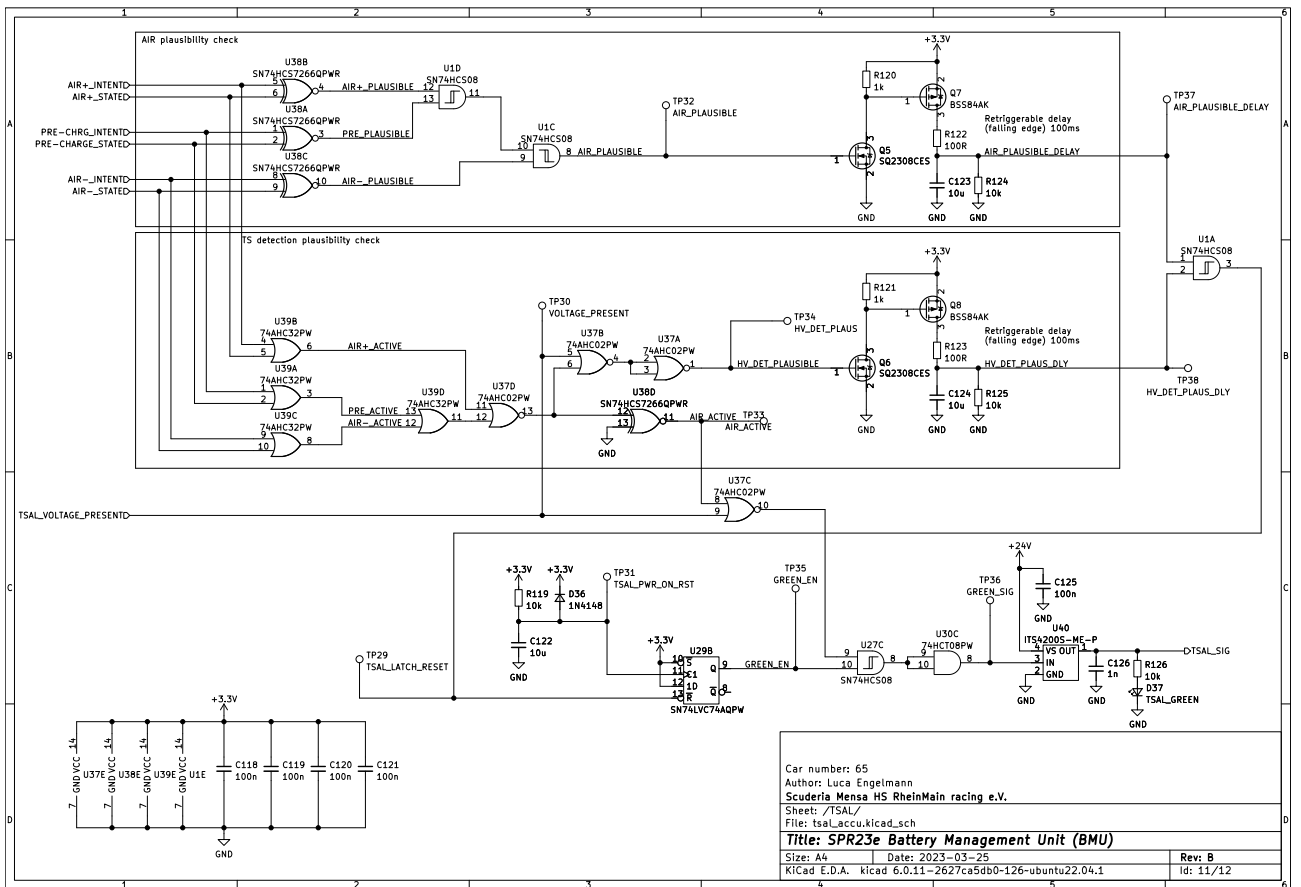


Figure 2.5.: Schematic of the TSAL accumulator logic.

The logic evaluates if the current state is plausible. A plausible state is always reached when the TSAC output voltage matches the relay state and if the actual relay state matches the intentional state. The truth table for the AIR plausibility check for each AIR is shown in Table 2.1. The resulting boolean function corresponds to an exclusive NOR gate (U38 in Figure 2.5).

Table 2.1.: Truth table for the plausibility check for each AIR.

AIR intentional	AIR actual	plausible	Comment
inactive	inactive	yes	No error
inactive	active	no	AIR stuck
active	inactive	no	State detection or coil wire broken
active	active	yes	No error

The AND gate U1 (Figure 2.5) combines the plausibility of all AIRs to one signal AIR_PLAUSIBLE, which is low as soon as one of the AIRs is implausible and high if all AIRs are plausible. A retriggerable delay circuit accommodates for the mechanical switching time of the AIRs. It delays the falling edge only and passes the rising edge through without any delay. The delay time is set by the time constant of C123 and



R124 (Figure 2.5) and the input threshold of the following AND gate (U1, Figure 2.5). The following gate needs to have Schmitt trigger inputs due to the slow falling edge caused by the delay. The input thresholds have a large tolerance and are not specified for a supply voltage of 3.3 V [8, Section 6.5]. The interpolated values for the negative threshold are $0.61 \text{ V} < U_{T-} < 1.22 \text{ V}$. At the maximum lower input threshold, the delay time is minimal and corresponds to the RC time constant τ . The circuit ensures a minimum delay time of 100 ms. At the minimum lower input voltage threshold, the delay time will increase to 170 ms.

The plausibility check for the TSAC output voltage detection uses both the intentional and the actual AIR states for comparison. U37 and U39 combine the six signals to one signal. If any of the AIRs is active (either intentional or unintentional) the signal AIR_ACTIVE will be high. The complex appearing connection of U37 and U38D results in an efficient utilization of the four independent gates within a package. U38D is configured to behave like an inverter. The signal HV_DET_PLAUSIBLE is a combination of the TSAC output voltage detection and the AIR state with the truth table shown below. The corresponding boolean function is an OR gate with one inverted input.

Table 2.2.: Truth table for the TSAC output voltage plausibility check.

Voltage present	AIR active	plausible	Comment
no	no	yes	No error
no	yes	no	Voltage detection broken wire
yes	no	yes	See text
yes	yes	yes	No error

A voltage greater than 60 V present at the TSAC output while no AIR is active is not considered as implausible since this happens on every discharge cycle. In this case, the green and the red LED of the TSAL will be active. This edge case is allowed by rule EV 4.10.6 and is thus not prevented. The HV_DET_PLAUSIBLE signal uses an identical retriggerable delay circuit. In this case, it is used to accommodate for the sum of the pre-charge time and the relay turn-on time. During pre-charge, the TSAC output voltage will rise depending on the time constant of the pre-charge resistor and the DC-Link capacitor. In order to detect a broken wire in the voltage detection circuitry, the plausibility check waits for the DC-Link voltage to rise above 60 V. This ensures that the broken wire is detected if the implausibility persists after the pre-charge time and pre-charging will not lead to a false triggering. The time it takes for the DC-Link voltage to rise above 60 V can be calculated with the basic capacitor charging formula shown in Equation 2.1.

$$U_c(t) = U_0 \cdot (1 - e^{-\frac{t}{\tau}}) \quad (2.1)$$

Re-arranging Equation 2.1 to solve for t is shown in Equation 2.2. The maximum t will be at the minimum battery voltage of 430 V. Solving for $U_c(t) = 60 \text{ V}$, $U_0 = 430 \text{ V}$, $\tau = RC = 1000 \Omega \cdot 300 \mu\text{F}$, Equation 2.2 yields:

$$t_{\text{pre}} = -\tau \cdot \ln \left(1 - \frac{U_c(t)}{U_0} \right) = -(1 \text{ k}\Omega \cdot 300 \mu\text{F}) \ln \left(1 - \frac{60}{430} \right) = 45 \text{ ms} \quad (2.2)$$

The turn-on time of the relays add to the pre-charge time. The resulting total pre-charge time $t_{\text{pre,sum}}$ equals:

$$t_{\text{pre,sum}} = t_{\text{on,relay}} + t_{\text{pre}} = 25 \text{ ms} + 45 \text{ ms} = 70 \text{ ms} \quad (2.3)$$

Therefore, a delay of 100 ms is sufficient as well.



The last section of the TSAL logic combines the plausibility check, the voltage detection signal, and the AIR_ACTIVE signal to control the green light of the TSAL. The flip-flop U29B is the latch required by EV 4.10.13 and EV 4.10.14. It is set on startup after a short delay, to ensure that all signals which clear the latch are stable. If the AIRs or the voltage detection are implausible, the latch is cleared. The output of the latch is used as enable signal for the green light. Therefore, the green light can only be activated, if the whole system is in a plausible state. The green light is then controlled by the AIR_ACTIVE and TSAL_VOLTAGE_PRESENT signal in a way that either of these signals turn off the green light. This ensures that the green light is deactivated as soon as at least one AIR is active and reactivated only if the voltage at the TSAC output is less than 60 V and all AIRs are off. The signal output uses the same method as described in subsection 2.3.2. The signal produced by U40 is directly routed to the TSAL lights.

2.3.5. Shutdown Circuit Control

The IMD and AMS must open the shutdown circuit in case of faults or critical values. EV 6.1.6 [1, p. 94] requires a non-programmable latch for this action. Figure 2.6 shows the schematic of the shutdown circuit latches. Once latched, they must only be manually reset as EV 6.1.6 requires [1, p. 93]. The latches will start in the cleared state on power-up. To avoid resetting the latches manually on power-up, an auto-reset circuit based on U1B, U2, and the surrounding components will clear the latches automatically after 3 s. U5 is reset-dominant as well. Therefore, the automatic reset will only work, if the IMD and AMS do not report any faults by pulling the IMD_STATUS or AMS_FAULT signals low. During the 3 s auto-reset, the manual reset buttons are disabled to allow for a self-check of the indicator LEDs required by T 11.9.5 [1, p. 59]. The auto-reset feature can be disabled, if required. The BMU sets an enable signal, which is used with U43A as a gate for the reset signal created by U2. U2 is needed to convert the inhibit-signal to a short pulse, which will set the latch. If the signal would be constantly active, the manual reset buttons could not be used anymore to set the latches, since the clock inputs of the latches are edge triggered. The indicator LEDs are driven by U6, which is a gate driver. Although not specifically designed to drive LEDs, it is a cheap and small solution which works flawlessly. The power stage for the shutdown circuit is comprised by Q2 and the surrounding components. D2 and D3 limit the gate-source voltage of the mosfets to safe values. Q1 and Q3 are used to control the power stage mosfets. The power stages are active, if the Q outputs of U5 are active. The negated outputs of U5 are used to drive the indicator LEDs and to feed the current state of the latches to the microcontroller.

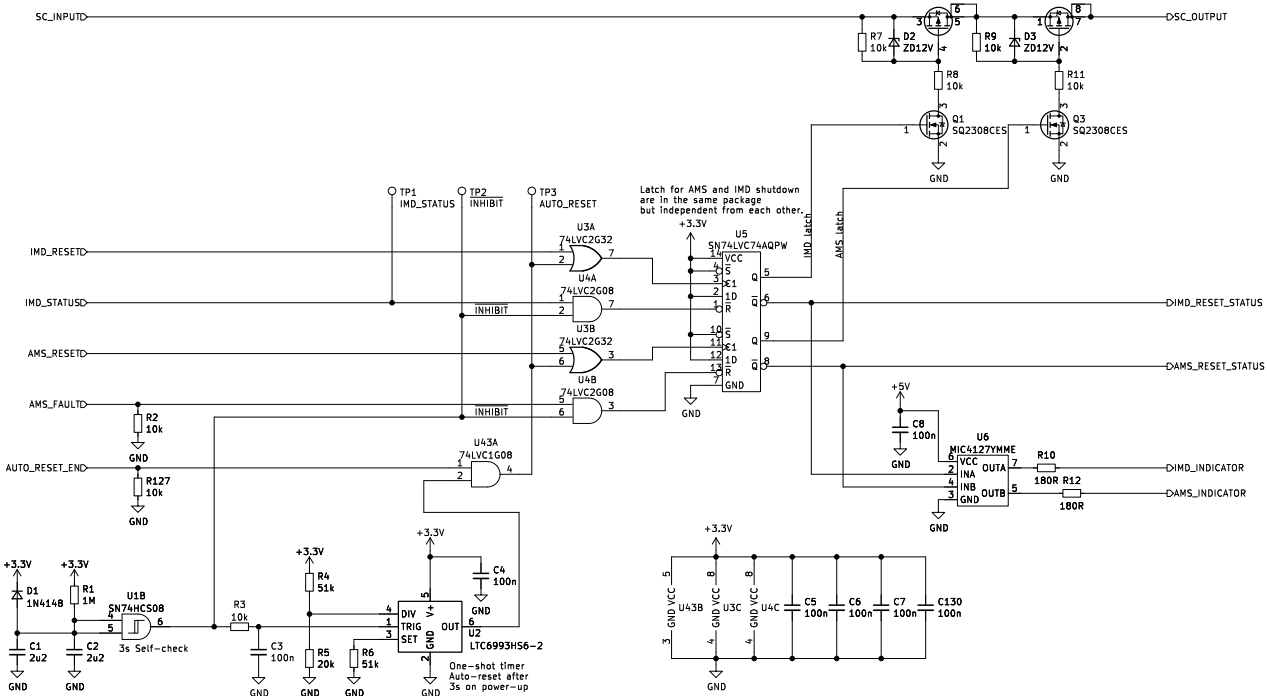


Figure 2.6.: Schematic of the shutdown circuit control.

2.3.6. Voltage Indicator driver

The voltage indicator is an LED located in the front of the accumulator container, indicating that the tractive system is active and high voltage is present at the output connector. It must be directly supplied from the tractive system, as EV 5.4.10 [1, p. 88] states. There are many different ways to power the LED, each with advantages and disadvantages. You could use a simple resistor. However, as Equation 2.4 shows, this solution would lead to a rather high power dissipation. Consider the following LED parameters: $U_f = 2\text{ V}$ and $I_f = 10\text{ mA}$. At maximum TS voltage the power dissipation would be:

$$P_d = (U_{TS,\max} - U_f) \cdot I_f = (600\text{ V} - 2\text{ V}) \cdot 0.01\text{ A} = 5.98\text{ W} \quad (2.4)$$

While this may be acceptable for applications where enough space for physically large resistors is available, for this application a more efficient but also more complex solution is chosen. The circuit is illustrated in Figure 2.7. The circuit is based around a VIPER012 (U35) off-line high voltage converter [9]. It is configured as a regulated step-down converter, which creates 24 V off of the tractive system voltage. It operates in a range of 50 V to 600 V and is based on the application note AN4858 [10]. It is slightly modified to meet the requirements. The original circuit is designed to be used with AC at the input. The rectification diodes at the input are removed, since they are not needed. The main filter capacitors C106 through C109 are rated for 400 V. Since 600 V capacitors in this capacitance range are not available, two 400 V capacitors are wired in series. To ensure equal voltage distribution across the two series capacitors, balancing resistors (R104 through R107 and R109 through R112, respectively) are used. The output voltage can be trimmed with the voltage divider R113 and R114 and is set to about 24 V, as Equation 2.5 [10, p. 6] shows:

$$U_o = U_{ref} \cdot \left(1 + \frac{R_{113}}{R_{114}}\right) = 1.2\text{ V} \cdot \left(1 + \frac{62\text{ k}\Omega}{3.3\text{ k}\Omega}\right) = 23.7\text{ V} \quad (2.5)$$



As the voltage across the inductor reaches a peak of approximately the input voltage during the on-state of the internal transistor of the VIPER012, the utilization of two inductors (L4 and L5) in series is employed. Note that special high voltage inductors are used here, which are specifically rated for an operating voltage of 400 V each [11, p. 1].

Since the voltage indicator has to be powered from the TSAC output (EV 5.4.8 [1, p. 88]), it must also work during the pre-charge period. This leads to a problem, however. The pre-charge path exhibits a relatively high impedance of $1\text{ k}\Omega$. Due to the loading effect of the startup current of U35 on the DC-Link, the voltage rise of the DC-Link is inhibited. To avoid this issue, the voltage indicator is powered from the TSAC output, as well as from the node between pre-charge resistor and pre-charge relay (see section 3.1). This allows the circuit to be powered from a low-impedance source during pre-charge. Both supply paths must be separated by ORing diodes D30 and D31.

To drive the LED galvanically isolated from the TS, an off the shelf isolated DC to DC converter (U36) is used. It will also further step the 24 V at the input down to 5 V at the output. The LED can directly be connected to the BMU, since the LED dropper resistor is equipped on the BMU (R118).

U35 exhibits an unstable behavior at an input voltage of about 30 V. The LED will start to pulse with a 1 Hz rate. To force a hard transition between on and off, the comparator circuit based around U34 is used. U34 is also directly powered from the TS using a zener diode to provide a stable supply voltage. To ensure minimal power dissipation in the dropper resistors R100 through R103, a comparator with very little power supply current is used. The LT6700 needs a maximum of $12.5\text{ }\mu\text{A}$ at a supply voltage of 12 V [12, p. 4]. It compares a fraction of the input voltage to an internal 400 mV reference voltage [12, p. 4]. The voltage divider R95 through R99 is designed to set the LED turn-on threshold to 55 V, as Equation 2.6 shows:

$$U_{\text{LED},\text{on}} = U_{\text{ref}} \left(1 + \frac{R_{95} + R_{96} + R_{97} + R_{98}}{R_{99}} \right) = 400 \text{ mV} \left(1 + \frac{1880 \text{ k}\Omega}{13.7 \text{ k}\Omega} \right) = 55 \text{ V} \quad (2.6)$$

At 600 V input voltage, the voltage at the input of U34 will be 4.34 V, which is well below the absolute maximum rating of 18.5 V [12, p. 2]. The open-collector output is used to drive a transistor (Q4), which will control the input of the isolated DC to DC converter. Although the LT6700 is a dual channel comparator, the second channel is not used. R108 adds some hysteresis to the comparator to yield defined threshold voltages (measured, including the tolerances of the parts) of 56 V (turn-on) and 40 V (turn-off).

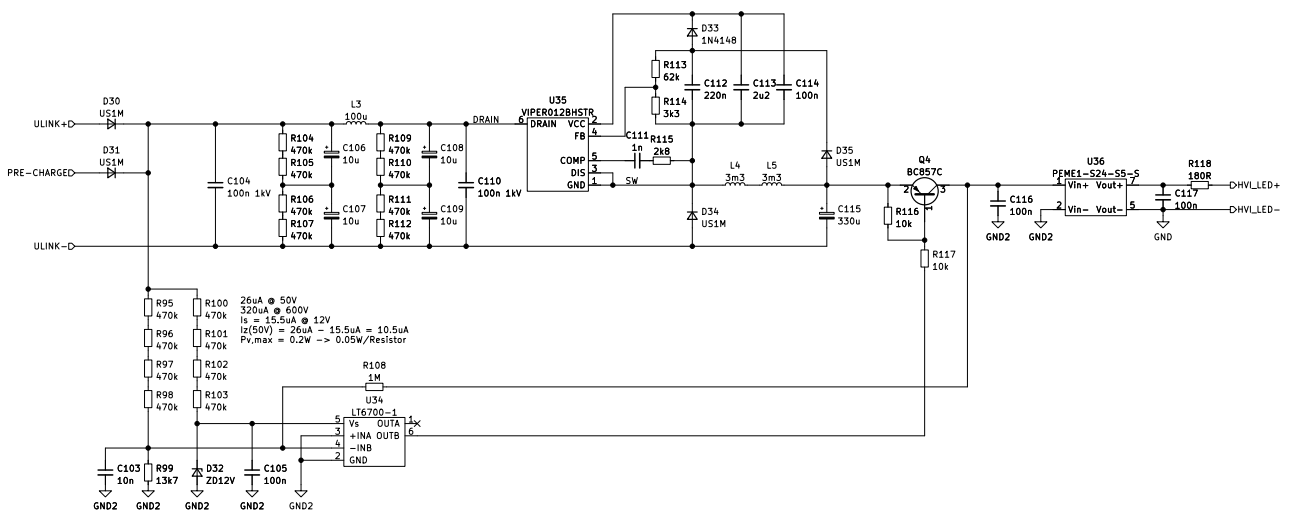


Figure 2.7.: Schematic of the voltage indicator driver.



2.3.7. Isolated TS voltage measurement

Figure 2.8 shows the schematic for the isolated tractive system voltage measurement. Both the battery voltage and the TSAC output voltage are measured using an identical circuit. Both channel are galvanically isolated with respect to the low-voltage system and each other. The isolation is performed in the analog signal chain with U20 and U21, respectively. U17 and U18 provide galvanically isolated power for the primary side of U20 and U21. C60 and C61 are used to reduce the common-mode noise generated by U17 and U18. The input voltage is divided with a factor of 301 to use the nominal input voltage range of the ACPL-C87B of 2V. This yields a measurement range of 602V. This utilizes the ACPL-C87B best and does not drive the following ADC with the full-scale input range. This leaves some headroom for calibration. The output of U20 and U21 is differential, which matches the differential inputs of the ADC. U23 acts as an active first-order low-pass filter to reduce high frequency chopper noise generated by U20 and U21 (Quelle). It also drives the input of the ADC and satisfies the maximum output load requirement of the ACPL-C87B. Since U23 is used in inverting configuration with a unipolar supply voltage, a common-mode voltage has to be added at the non-inverting input. By using half of the ADC's reference voltage, the full input voltage range of the ADC can be used. Additional to the voltage measurement, a voltage check is implemented at the TSAC output. This is used for the TSAL logic and outputs a binary signal. The output is logically high if a voltage greater than 52 is present at the TSAC output. The optocoupler U22 is used for galvanic isolation. U19 is used as comparator with an internal reference voltage of 2.5V.

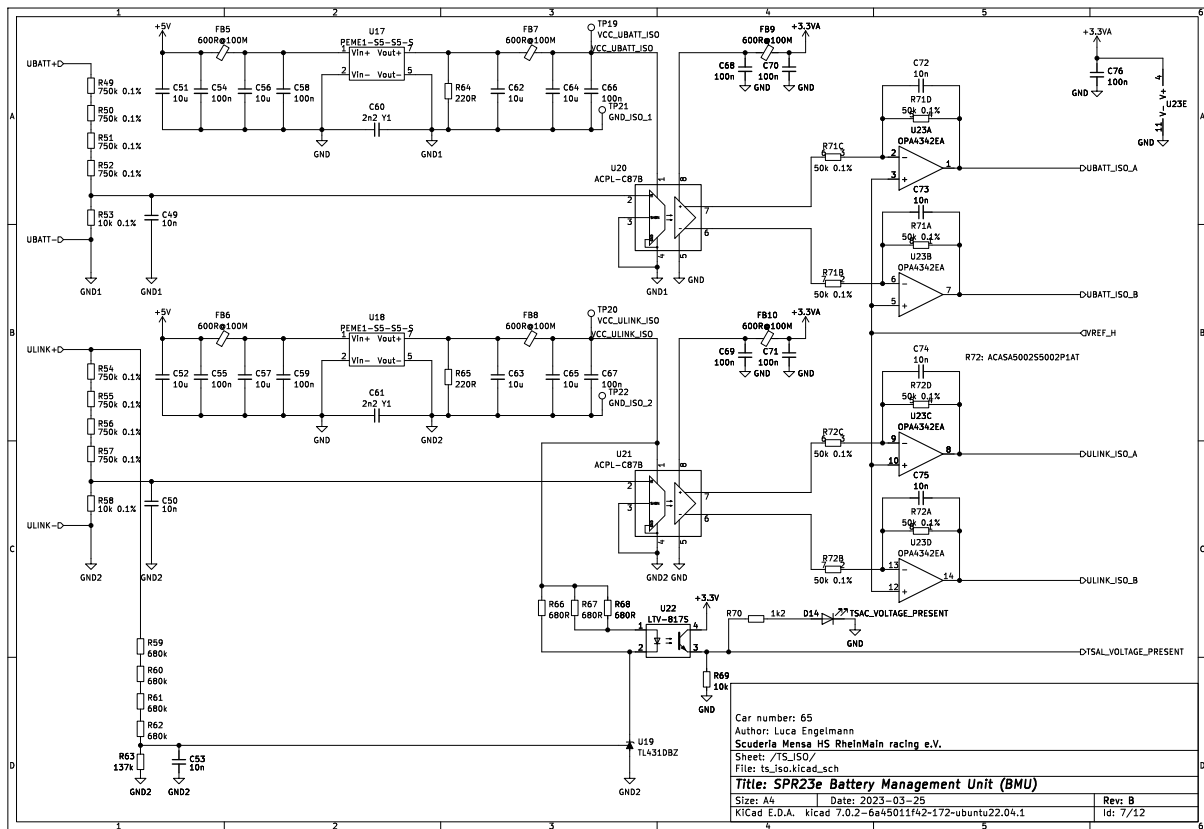


Figure 2.8.: Schematic of the isolated TS voltage measurement and voltage detection for the TSAL.



2.3.8. ADC

Accuracy specification

Figure 2.9 shows the block diagram of the isolated voltage measurement described in subsection 2.3.7. Each stage in the signal chain introduces some form of measurement error. This section will characterize the system and calculate the measurement error. The error introduced by each stage is shown in Table 2.3. While some of these errors can be removed by calibrating the system, others cannot. Due to their dynamic behavior over temperature or input voltage, a static calibration is not sufficient to remove these types of errors. For any temperature dependent variable in Table 2.3, a maximum temperature of 60 °C is to be assumed. The reference temperature is 25 °C. Each value is given as a percentage value related to the nominal input voltage range of the ACPL-C87B, which is 2 V. For temperature dependent values, the value at maximum temperature is given.

Table 2.3.: Sources of error in each stage of the analog signal chain, type of error, and ability for correction.

Stage	Error source	Error type	Value	Correctable
Voltage divider	Tolerance	Gain error	0.200 %	Yes
	Drift	Gain error	0.200 %	No
Isolator	Offset error	Offset error	0.500 %	Yes
	Gain error	Gain error	0.500 %	Yes
	Nonlinearity	Gain error	0.120 %	No
	Offset drift	Offset error	0.042 %	No
	Gain drift	Gain error	0.100 %	No
	Noise	Offset error	0.065 %	No
ADC driver	Offset error	Offset error	0.300 %	Yes
	Gain error	Gain error	0.100 %	Yes
	Offset drift	Offset error	0.006 %	No
	Gain drift	Gain error	0.200 %	No
ADC	Offset error	Offset error	0.045 %	Yes
	Gain error	Gain error	3.000 %	Yes
	Offset drift	Offset error	0.000 %	No
	Gain drift	Gain error	0.008 %	No
	Nonlinearity	Gain error	0.001 %	Yes
Reference	Tolerance	Gain error	0.050 %	Yes
	Drift	Gain error	0.120 %	No

The overall measurement error is usually given as $\pm(\% \text{ of displayed value} + \% \text{ of range})$. The first term expresses the gain error, the second term the offset error. The overall error can be calculated by summing all similar errors to yield a worst-case estimation. A more statistical analysis uses the root-sum-square (RSS) method, that assumes that the actual error is near the center of the tolerance range instead of near the tolerance limits. The RSS method can be expressed with the following formula:

$$\sigma = \sqrt{\sum_{i=1}^n \sigma_i^2} \quad (2.7)$$



Table 2.4 shows the unadjusted error with the worst-case and RSS method, as well as the adjusted error with both methods. The RSS method after calibration is used to specify the accuracy. The overall accuracy satisfies the requirements.

Table 2.4.: Unadjusted and adjusted measurement error of the tractive system voltage measurement using the worst-case and root-sum-square method.

	Sum	$\pm(4.60\% + 0.96\%)$
Unadjusted	RSS	$\pm(3.07\% + 0.59\%)$
Adjusted	Sum	$\pm(0.75\% + 0.11\%)$
	RSS	$\pm(0.34\% + 0.08\%)$

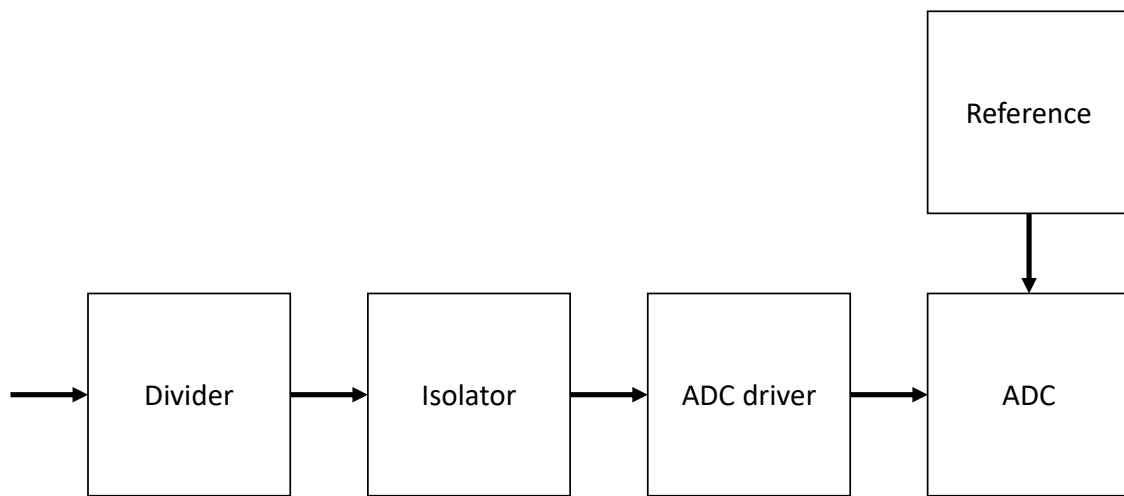


Figure 2.9.: Block diagram of the voltage measurement.



3. Battery Disconnect Unit

The Battery Disconnect Unit (BDU) contains the AIRs, the main TS fuse, the current sensor, and the rest of the battery electronics. Figure 3.1 shows the schematic of the accumulator electronics. The BDU is separated into two compartments. One compartment contains the TS components, the other compartment contains the BMU and IMD. The BDU is a 3D printed part using UL94-V0 compliant PETG filament with the minimum required wall thickness to satisfy the EV 5.5.3 [1, p. 89] and T 1.2.1 [1, pp. 22] rules respectively.

3.1. AIR PCB

The AIR PCB is directly screwed on top of the AIRs to supply fused measuring points to the BMS and IMD. It also allows the use of tab washers to secure the bolts with a positive locking mechanism, as required by EV 4.5.14 [1, p. 83]. FR4 is also the only exception of compressible material within the stackup of the TS connection as EV 4.5.12 states [1, p. 82]. Figure 3.2 shows the schematic of the AIR PCB. As described in subsection 2.3.6, the voltage indicator is both driven from the TSAC output on the vehicle side of the AIRs and from the junction between pre-charge resistors and pre-charge relay. Notice that K3 in Figure 3.2 is mirrored, since the TE LEV100 contactors have a preferred current direction for increased life span.

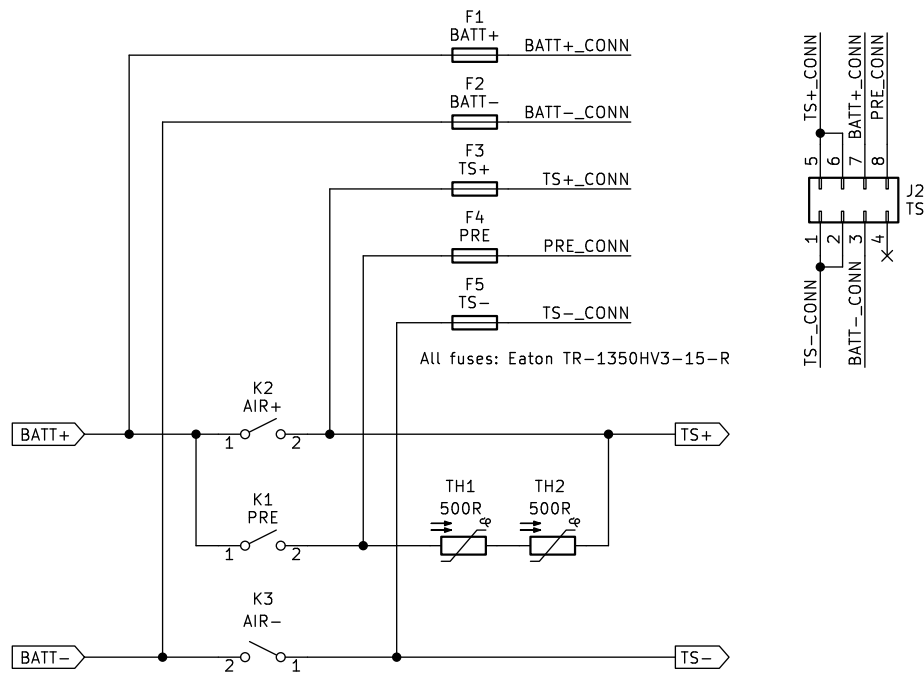
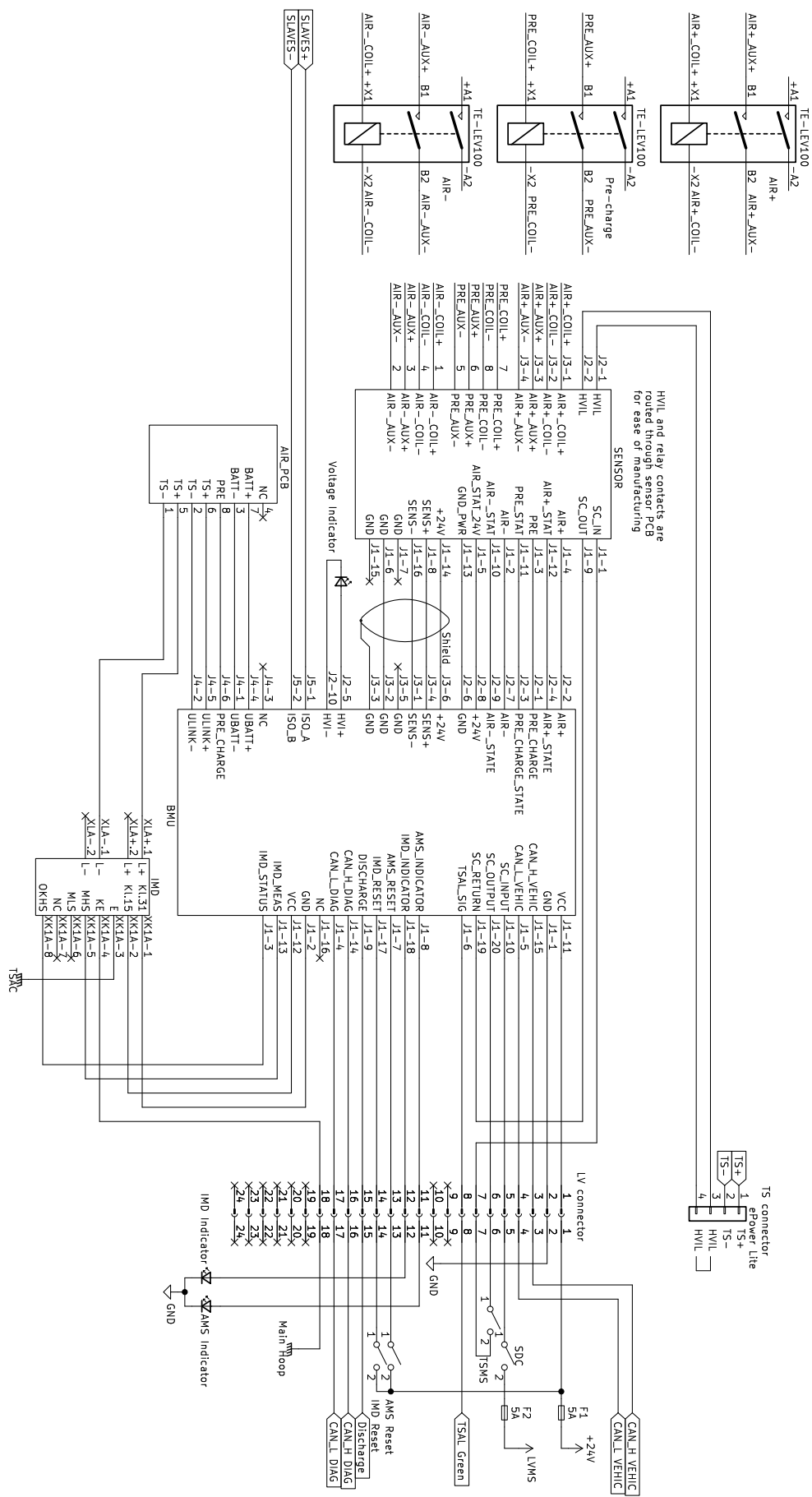


Figure 3.2.: Schematic of the AIR PCB



Figure 3.1.: Schematic of the accumulator electronics inside the Battery Disconnect Unit.





3.2. Current Sensor

Schaltplan, Beschreibung der Komponenten, Berechnung der Genauigkeit und Rendering



4. Software Architecture

Softwarearchitektur erläutern

4.1. <Software Modul>

Softwaremodule erläutern



5. Test and Validation

5.1. Test Setup

Testaufbau erklären

5.2. TSAL Test

The TSAL accumulator logic has been simulated with LTSpice before putting it onto the PCB. The simulation tests all possible error conditions, including stuck relays, broken relay state detections and a line break in the voltage detection. The simulation results have been checked against the real behavior using a Hardware-in-the-loop (HIL) test procedure. A S32K144-Q100 evaluation board [13] is connected via CAN to the BMU and controls the relays in the test setup based on the commands sent by the BMU. It also feeds back the current state of the TSAL signal. The BMU runs a modified firmware which contains the test procedures. These tests can be initiated via the UART interface. During the test, the BMU will output all necessary values in CSV format over the UART interface in 50 ms time intervals. The BMU firmware uses the measured DC-Link and battery voltages to perform the pre-charge. The simulation performs the pre-charge using a constant timing for the relays. Stuck relays may lead to different pre-charge times than usual. The simulation will not account for that fact. However, it does not influence the behavior of the TSAL logic. Furthermore, the slow appearing rise and fall times in the test results are an artifact from the 50 ms time slices. They do not represent the real rise and fall times. Another artifact from the same source are shifted edges by ± 50 ms. The following pages show the simulation result on the left side and the real behavior on the right side in the following order:

1. No error
2. Positive AIR stuck
3. Pre-charge relay stuck
4. Negative AIR stuck
5. Voltage detection broken wire
6. Positive AIR state detection broken wire
7. Pre-charge relay state detection broken wire
8. Negative AIR state detection broken wire

The graphs in each plot represent the logic signals at the most important points in the circuit. The upper most plot shows the output of the TSAL logic, which controls the green light. The second graph shows the voltage detection with a logical high at 3.3 V representing a detected voltage > 60 V. The relay intent and state plots are self explanatory. They represent the intentional and actual state of the relay with a logical high representing an active state. The last plot shows the DC-Link voltage measured by the BMU. The simulation uses the accumulator voltage of 600 V while the HIL test uses 24 V. The plots of the HIL tests use 0 and 1 to denote the logical states.



Test 1: No error

In this test, the BMU performs a pre-charge and a discharge cycle. The TSAL green light shall turn off, as soon as at least one AIR is closed or the voltage across the DC-Capacitor is greater than 2.5 V and shall turn back on, if all AIRs are open and the DC-Link voltage is less than 2.5 V. The 24 V/2.5 V ratio between the battery voltage in the test setup and the TS detection threshold is approximately the same as in the real setup with a ratio of 600 V/60 V. As seen in Figure 5.2, the TSAL logic behaves exactly as simulated. The test would not be passed, if the LED would not turn off at the 1 s mark or would remain off at the 4.4 s mark.

Test 2: Positive AIR stuck

This test simulates a stuck positive AIR. The AIR+ state is therefore always high. During pre-charging, the negative AIR closes. Therefore, the pre-charge resistor is bridged in this scenario. Notice that the simulation uses a simple time-controlled pre-charging while the real BMU performs the pre-charging based on the DC-Link and battery voltage. This explains the short on-time of the pre-charge relay compared to the simulation due to the fast rise time of the DC-Link voltage. Notice also, that the BMU with the final firmware would not allow to close any relay if one of the relay is stuck. Both the simulation in Figure 5.3 and the HIL test in Figure 5.4 show, that the TSAL green light never turns on, as required.

Test 3: Pre-charge relay stuck

A stuck pre-charge relay does not directly lead to malfunction of the pre-charge sequence or the general function of the tractive system. However, it would violate EV 5.6.2 [1, p. 90]. A stuck pre-charge relay is detected correctly as Figure 5.5 and Figure 5.6 show. The TSAL's green light does not turn on at all.

Test 4: Negative AIR stuck

Similarly to test 3, a stuck negative AIR causes no direct malfunction of the system but it will also violate EV 5.6.2 [1, p. 90]. This fault is correctly detected as well, as seen in Figure 5.7 and Figure 5.8.

Test 5: Voltage detection broken wire

A broken wire or blown fuse in the voltage detection circuit is simulated in this test. Since the voltage detection circuit and the TSAC output voltage measurement share the same wire and fuse, the DC-Link voltage and the voltage detection in both the simulation and the real hardware read always zero. Additionally, since the simulation does not use the DC-Link voltage to perform the pre-charge, the relay sequence looks identical to any other test (Figure 5.9). The BMU will remain in the pre-charge state since the DC-Link voltage does not reach 95 % of the battery voltage, causing the positive AIR to never energize (Figure 5.10). It is apparent that as soon as the negative AIR and the pre-charge relay turn on, the green light turns off and remains off, after both relays de-energize again.



Tests 6, 7, and 8: Relay state detection broken

Due to their similarities, the last three tests are summarized here. As seen in Figure 5.12, Figure 5.14, and Figure 5.16, the state detection of the positive AIR, pre-charge relay, and negative AIR read constantly zero. This fault is detectable, as soon as the corresponding relay is energized. The green light turns off, as soon as the AIRs are energized and remains off after the relays de-energize due to the fault latching.

TSAL Test: Summary

In summary, the tests show that the TSAL accumulator logic recognizes all possible faults correctly and behaves rule compliant. While these tests seem extremely elaborate and time-consuming, it is important to fully validate the functionality of the TSAL logic, since it is a safety-critical part that must behave under all circumstances as expected.

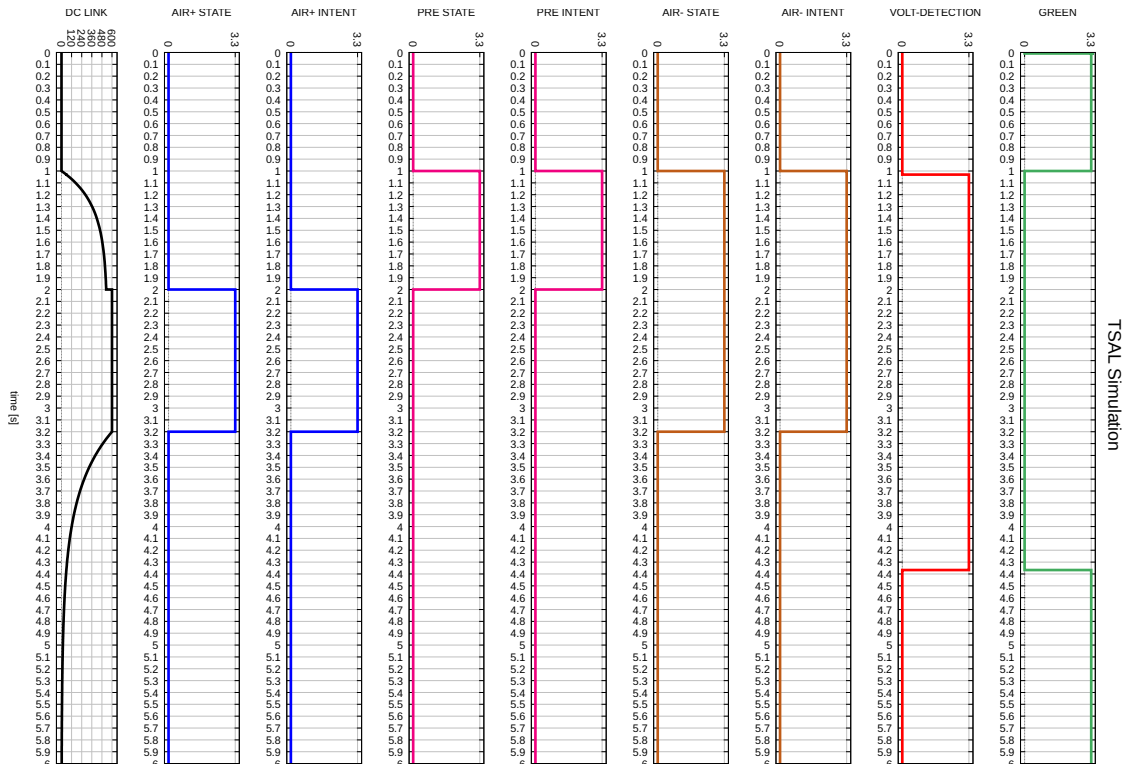


Figure 5.1.: TSAL simulation result. Test: No errors.

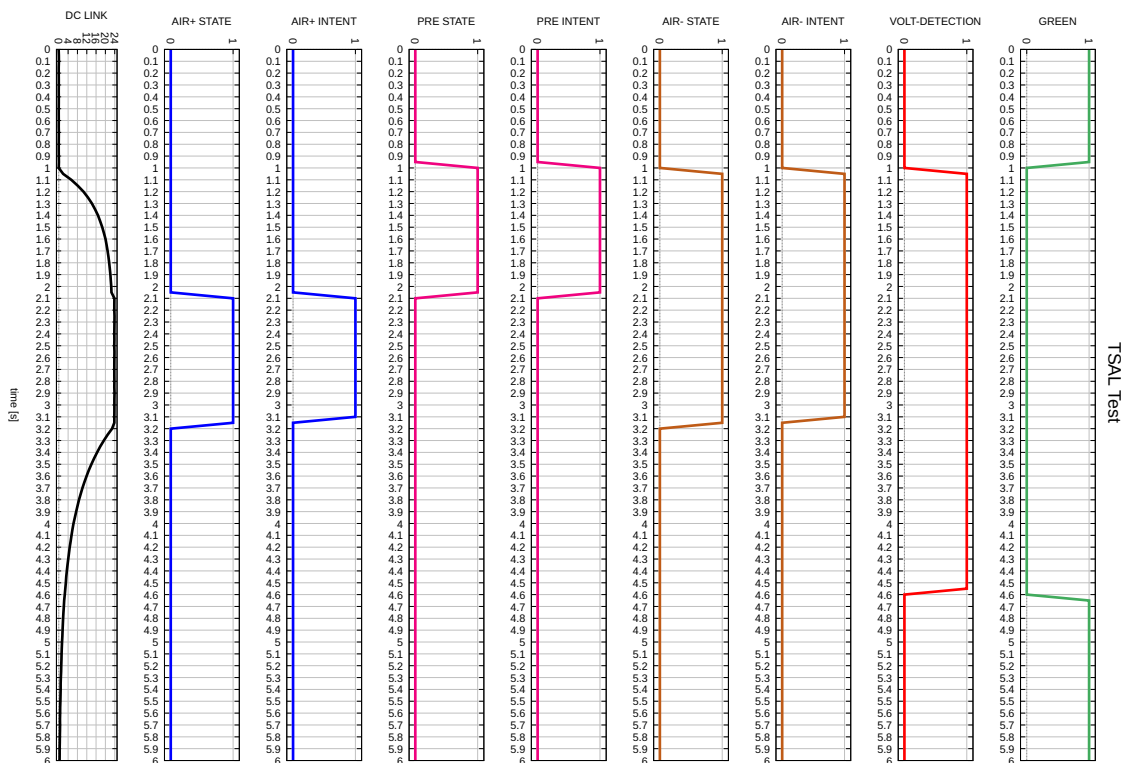


Figure 5.2.: TSAL HIL result. Test: No errors.

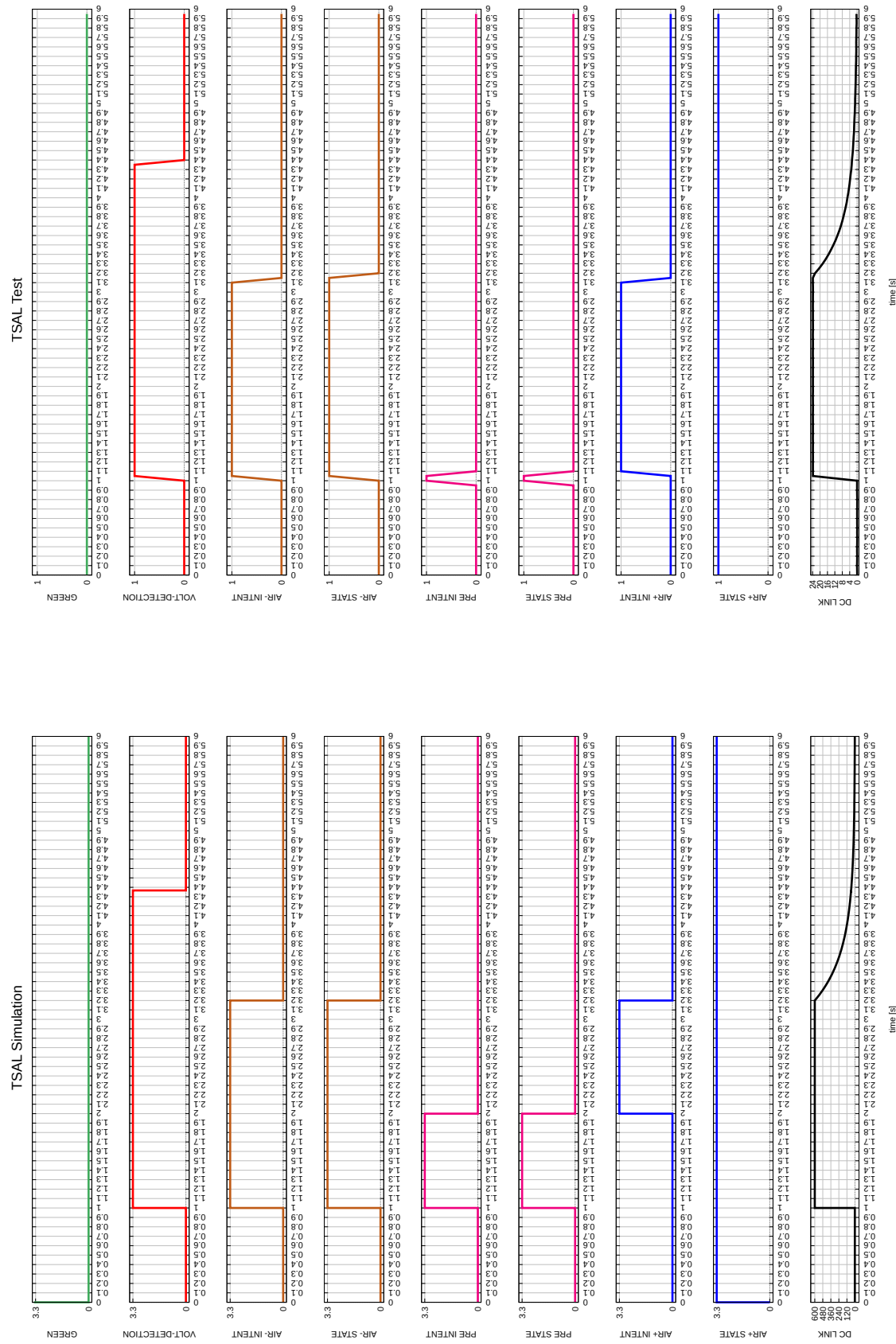


Figure 5.3.: TSAL simulation result. Test: Positive AIR stuck.

Figure 5.4.: TSAL HIL result. Test: Positive AIR stuck.

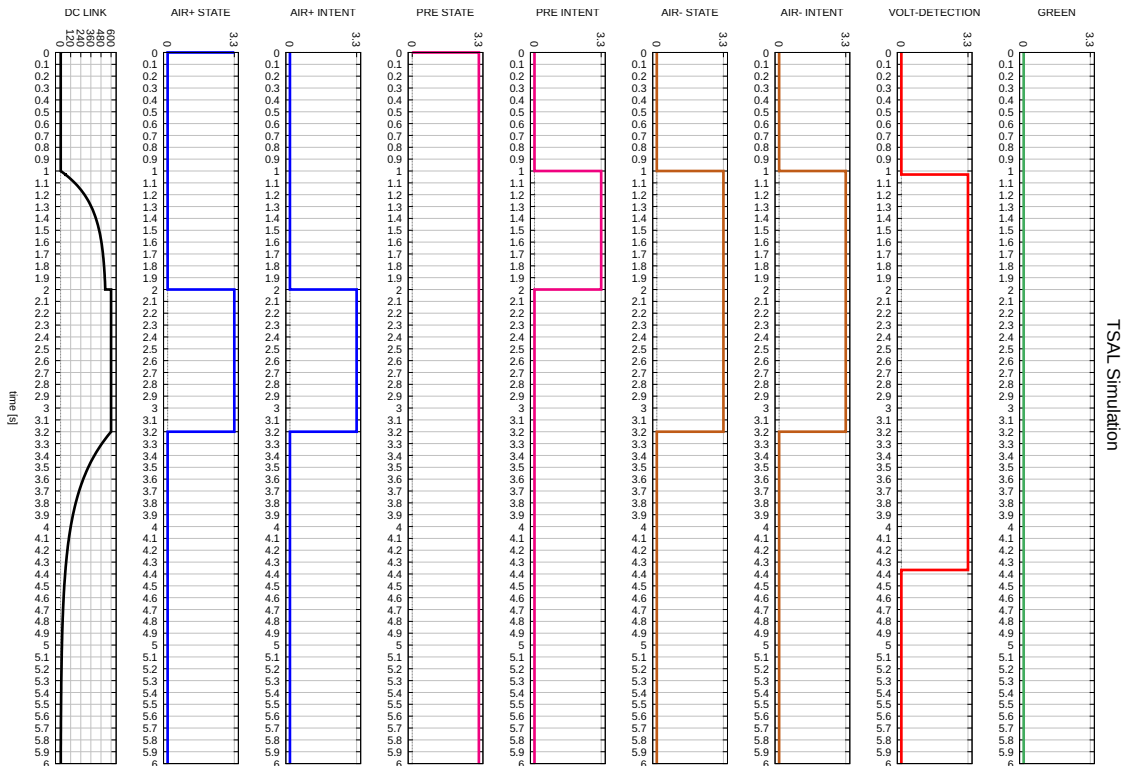


Figure 5.5.: TSAL simulation result. Test: Pre-charge relay stuck.

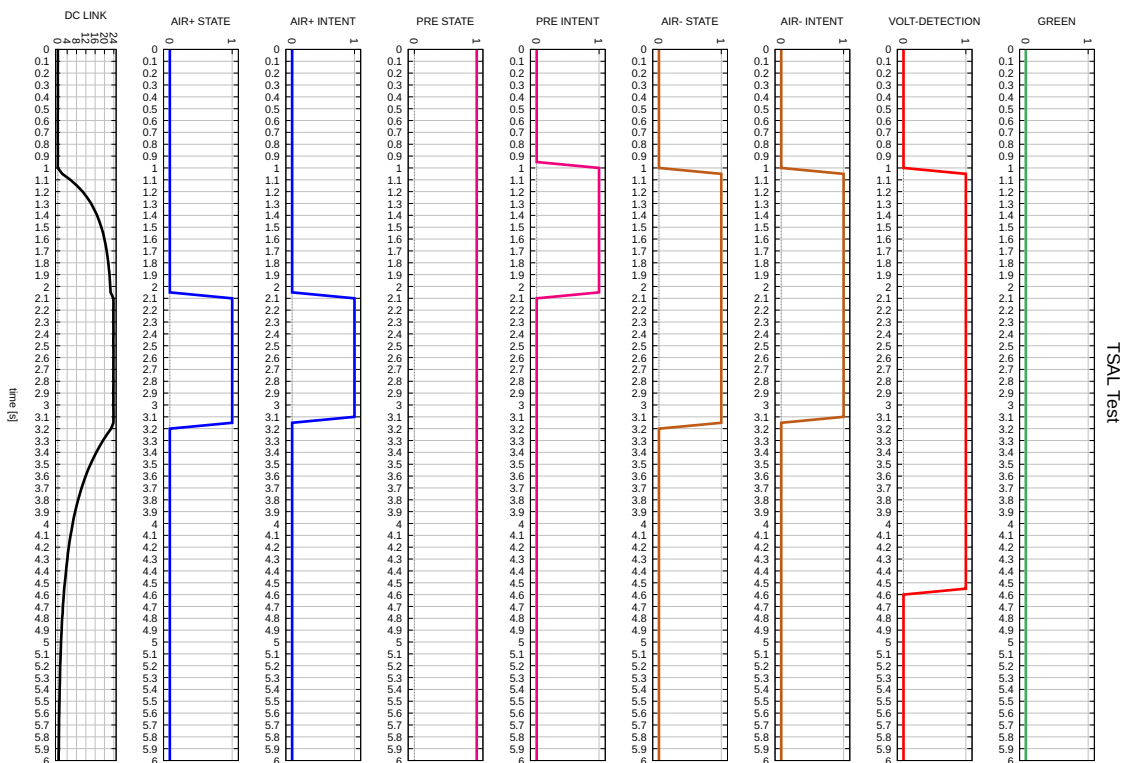


Figure 5.6.: TSAL HIL result. Test: Pre-charge relay stuck.

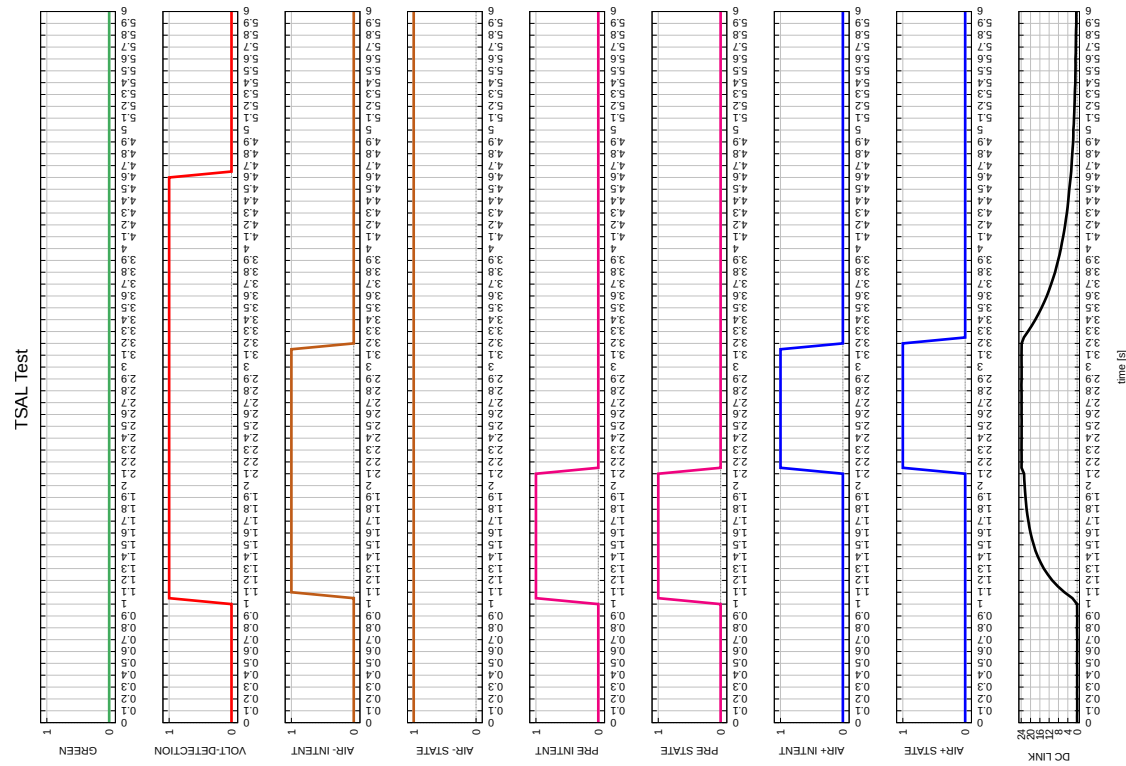


Figure 5.8.: TSAL HIL result. Test: Negative AIR stuck.

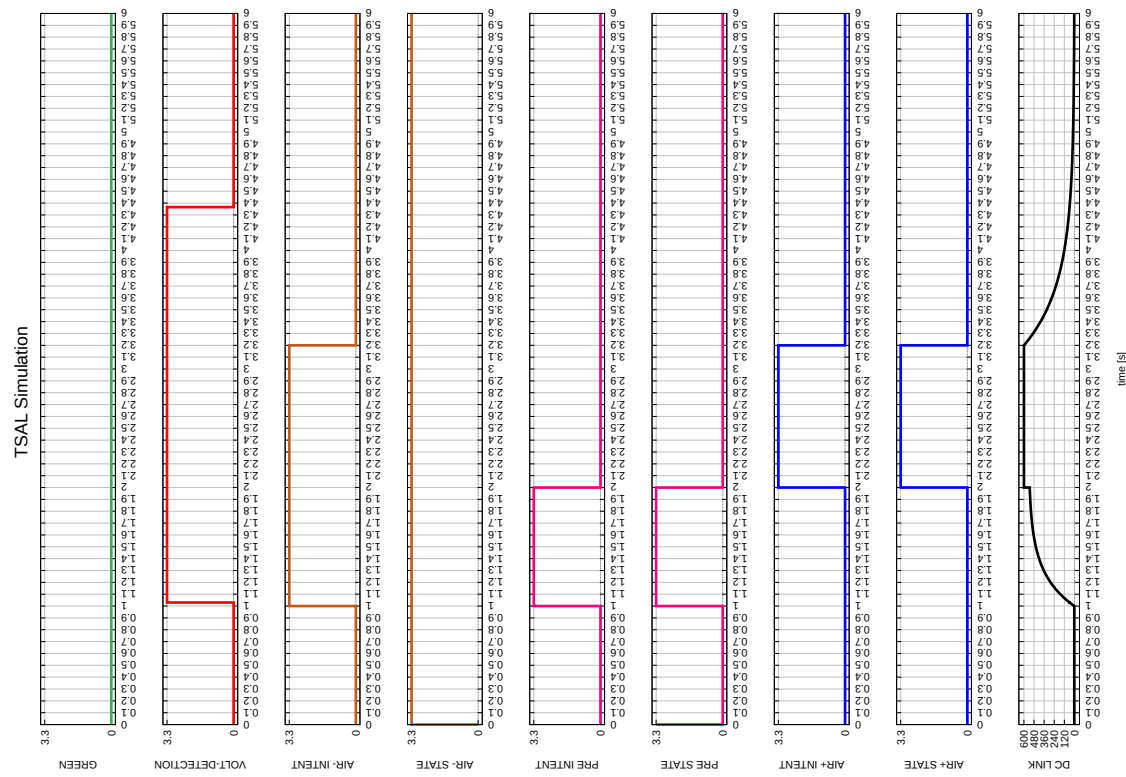


Figure 5.7.: TSAL simulation result. Test: Negative AIR stuck.

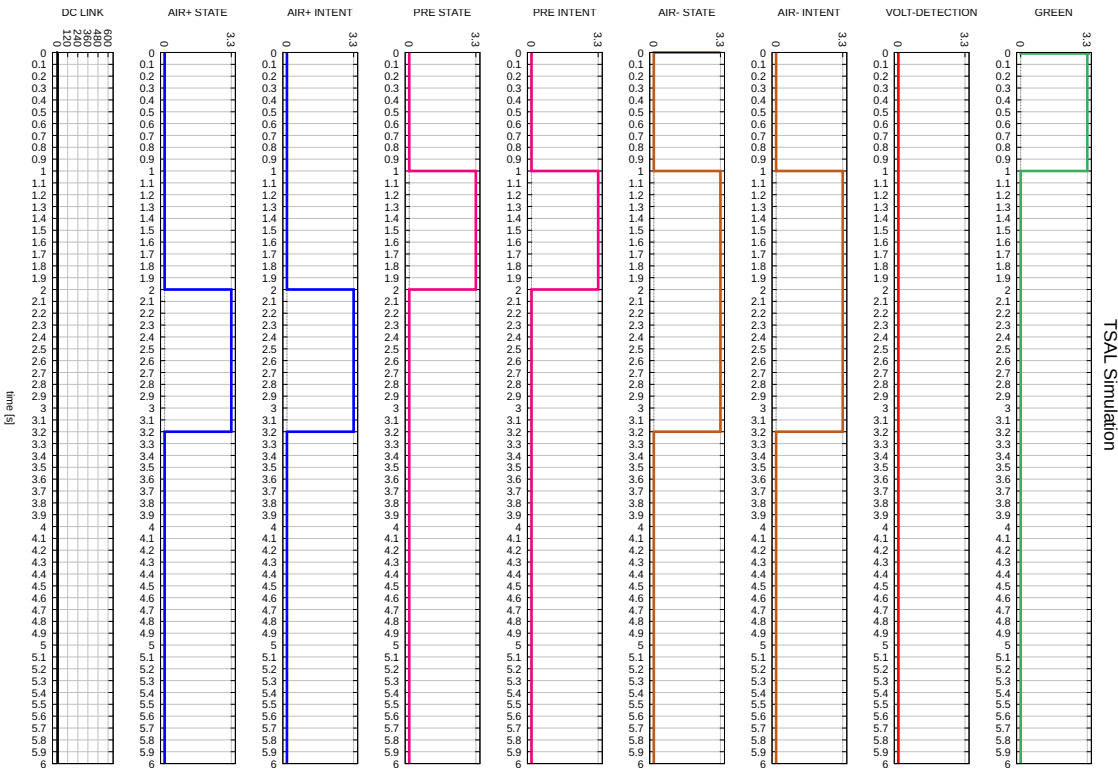


Figure 5.9.: TSAL simulation result. Test: Voltage detection broken wire.

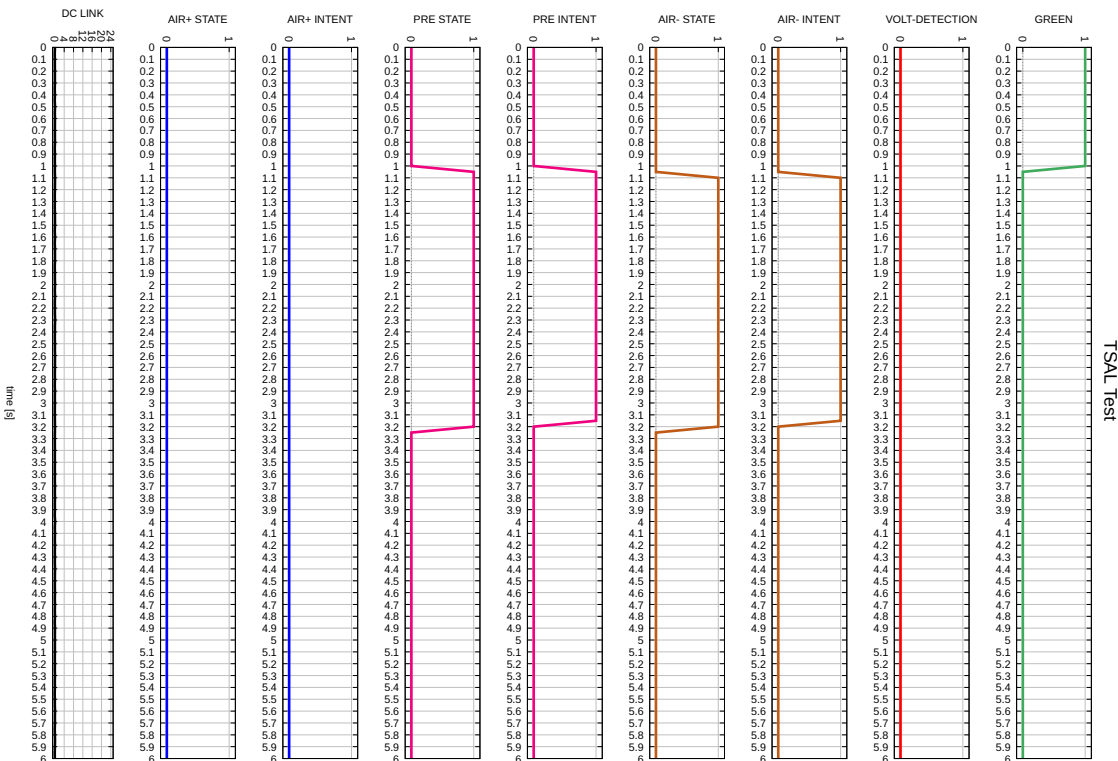


Figure 5.10.: TSAL HIL result. Test: Voltage detection broken wire.

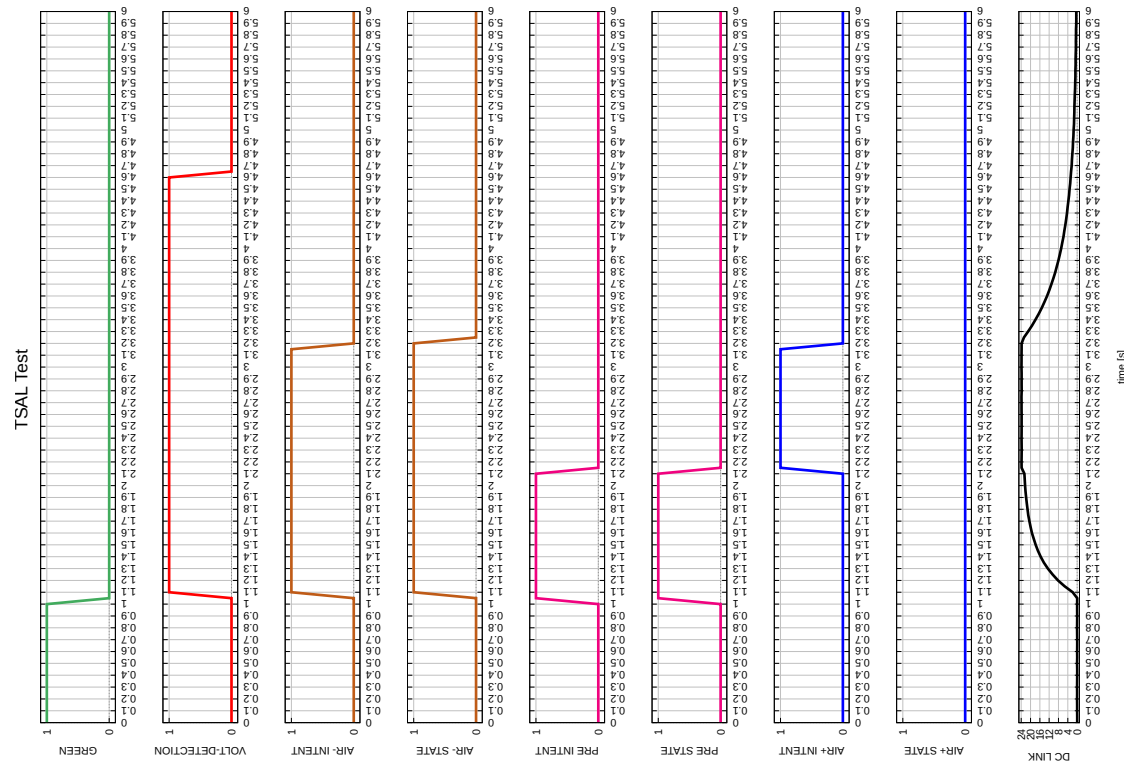


Figure 5.12.: TSAL HIL result. Test: Positive AIR state detection broken wire.

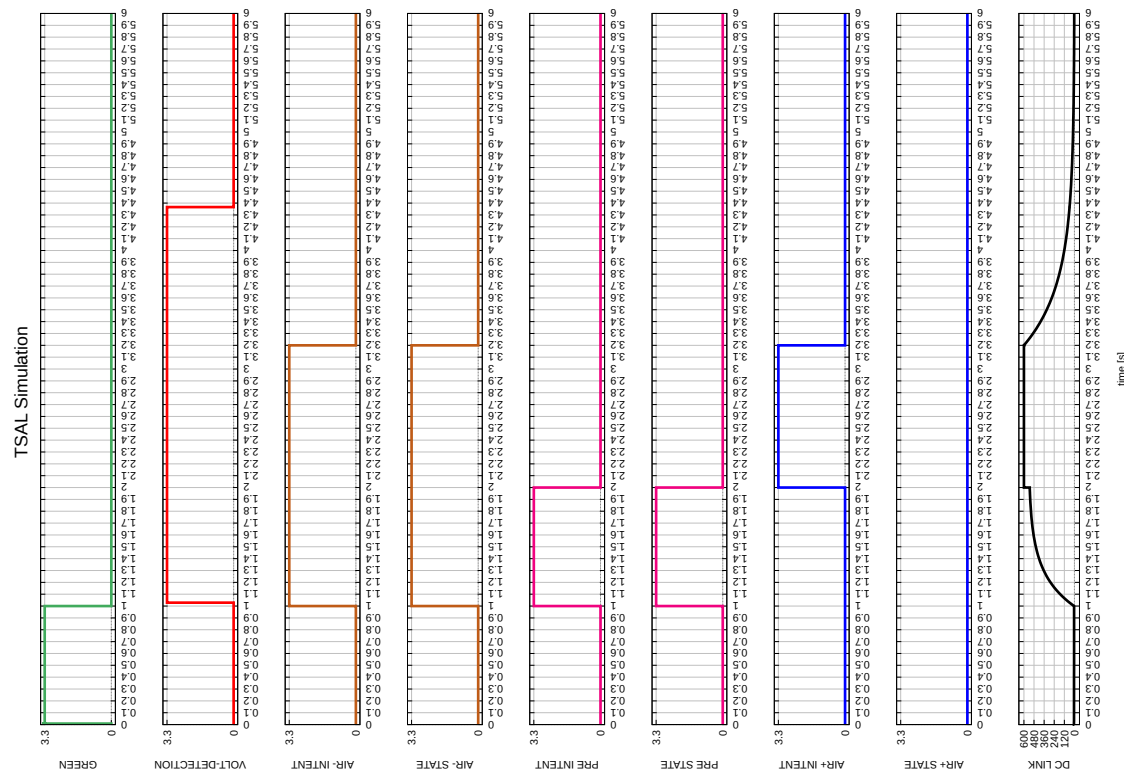


Figure 5.11.: TSAL simulation result. Test: Positive AIR state detection broken wire.

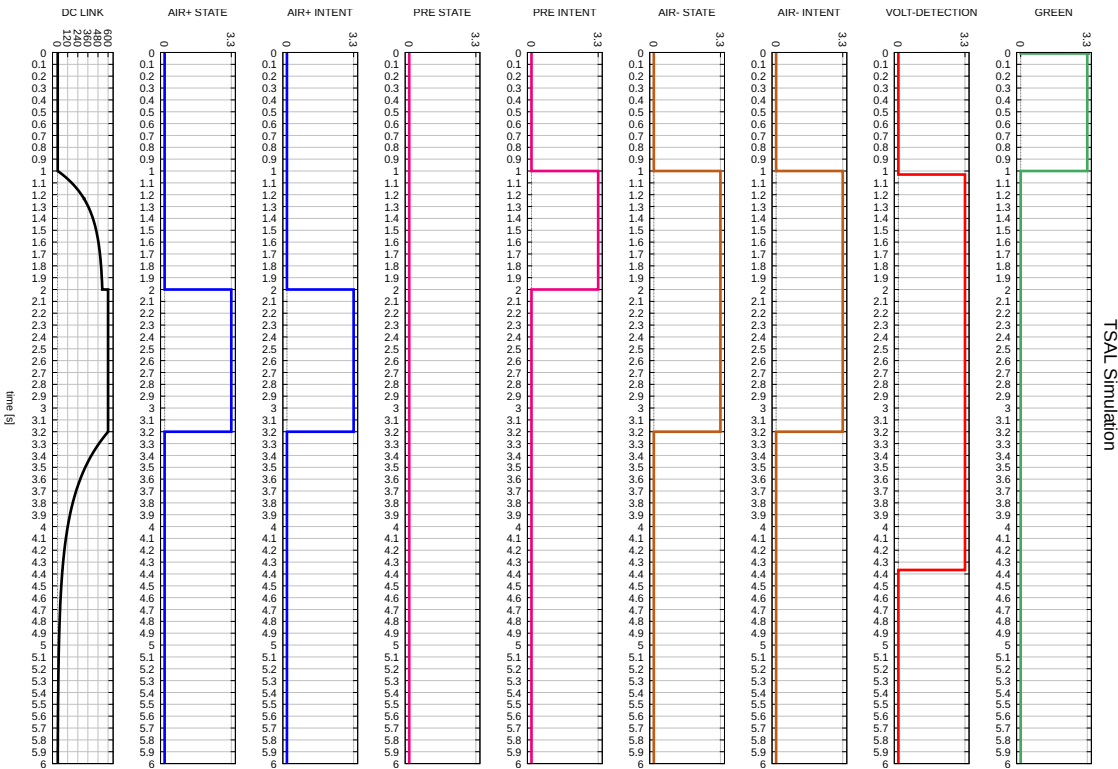


Figure 5.13.: TSAL simulation result. Test: Pre-charge relay state detection broken wire.

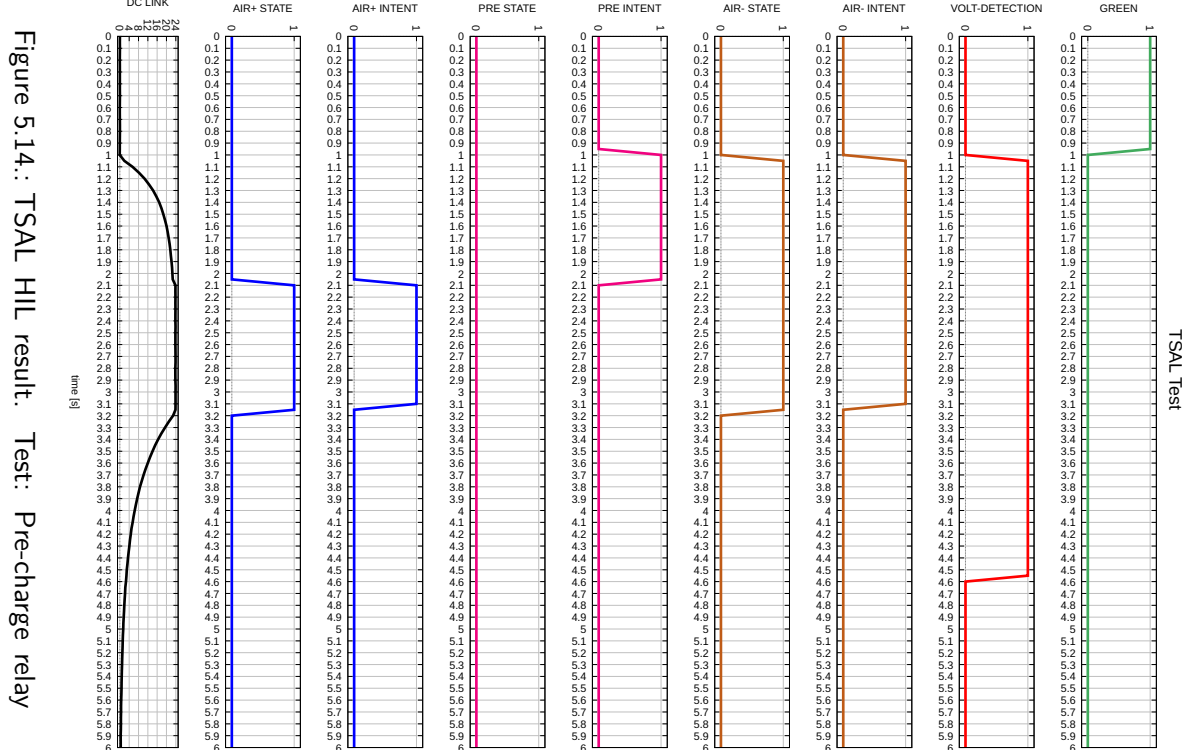


Figure 5.14.: TSAL HIL result. Test: Pre-charge relay state detection broken wire.

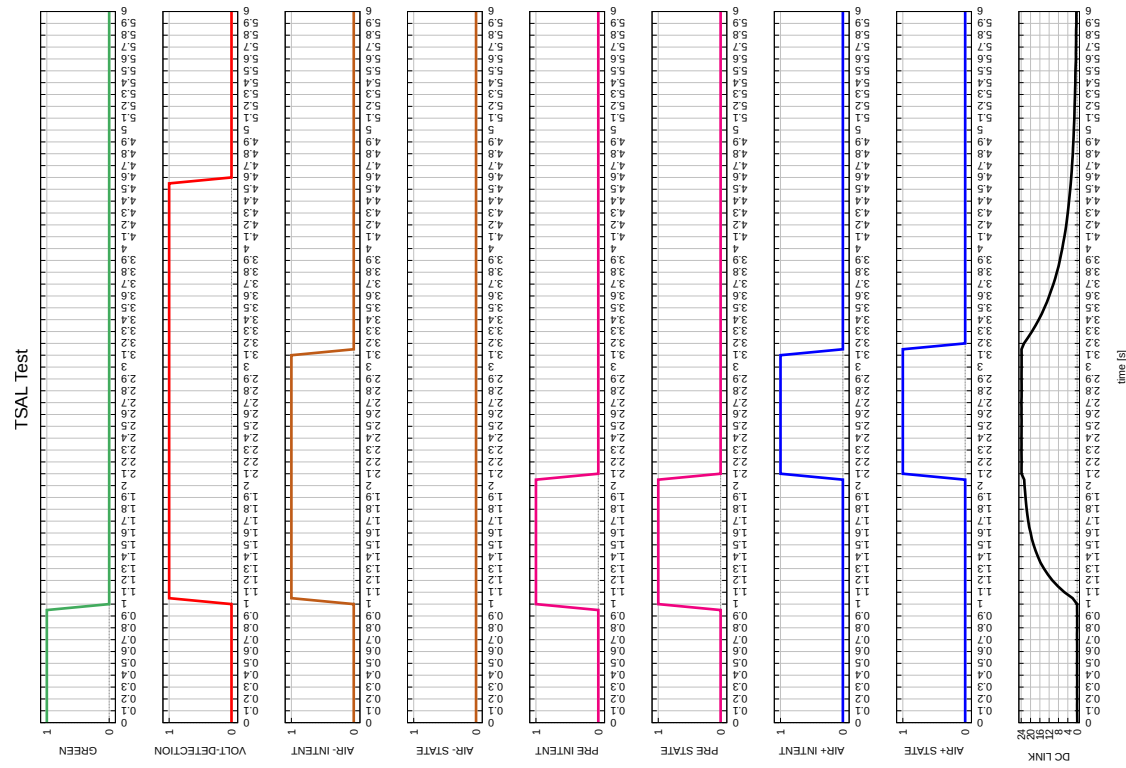


Figure 5.16.: TSAL HIL result. Test: Negative AIR state detection broken wire.

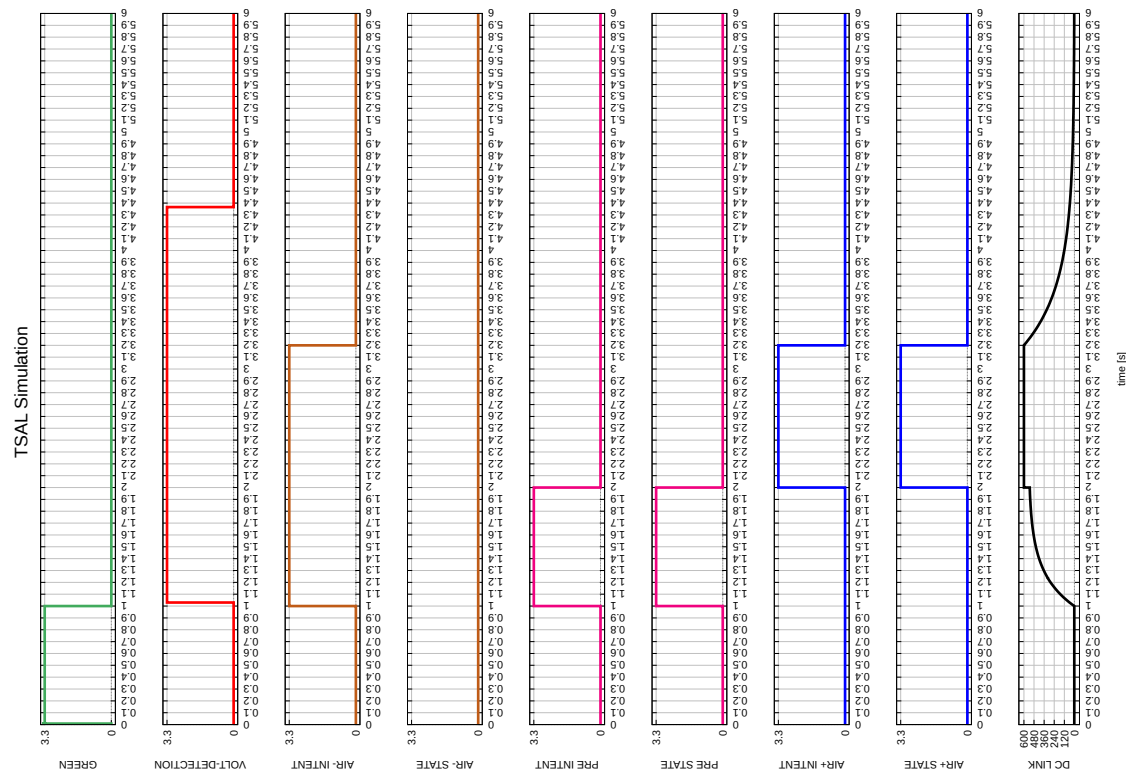


Figure 5.15.: TSAL simulation result. Test: Negative AIR state detection broken wire.



6. Potential Improvements

Mögliche Verbesserungen



7. Bibliography

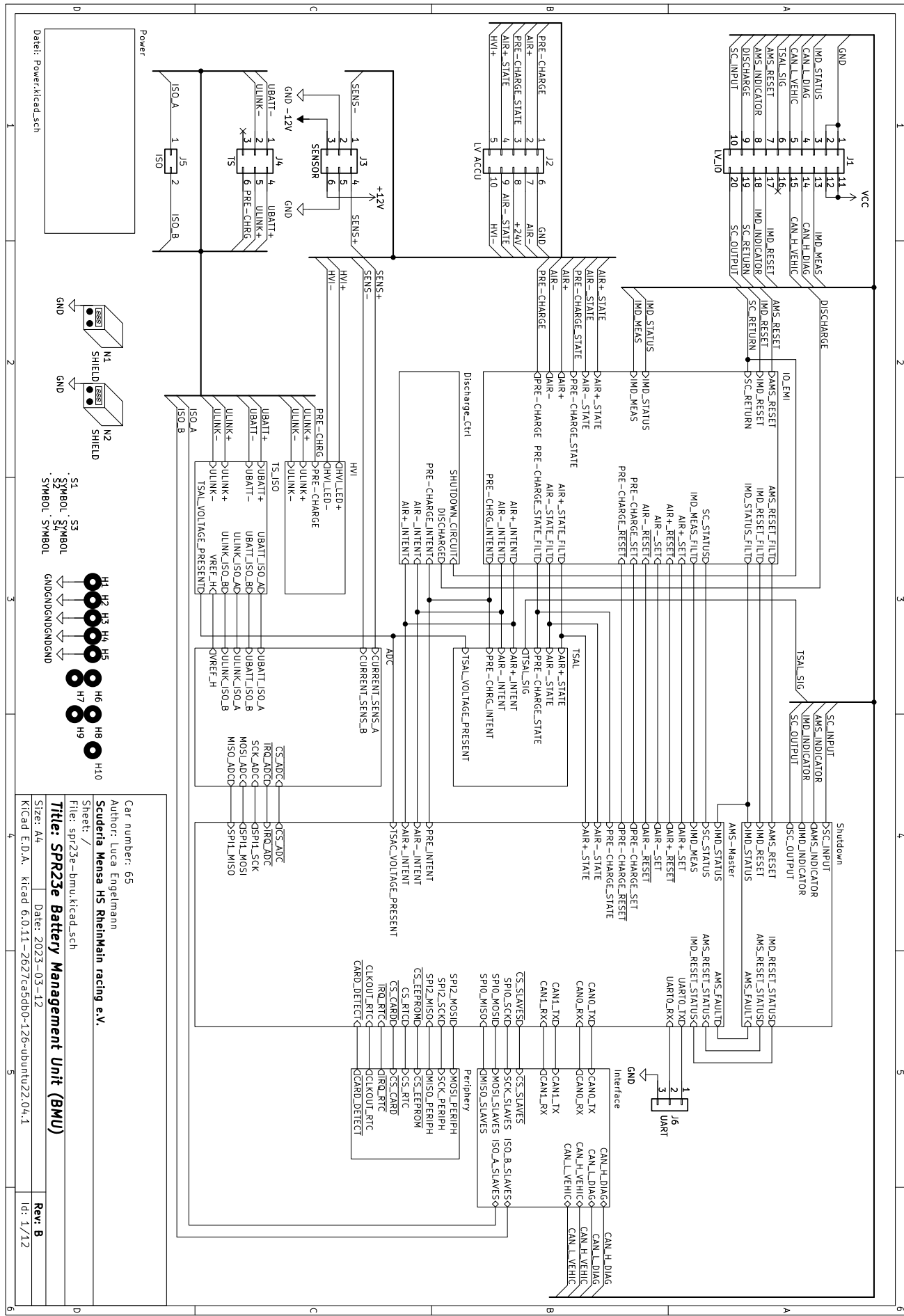
- [1] *Formula Student Rules 2023*, Formula Student Germany, 2023, Version 1.1. [Online]. Available: https://www.formulastudent.de/fileadmin/user_upload/all/2023/rules/FS-Rules_2023_v1.1.pdf [Accessed: 2023/03/19]
- [2] J. Munson, "Low Cost isoSPI Coupling Circuitry for High Voltage High Capacity Battery Systems." [Online]. Available: <https://www.analog.com/en/technical-articles/low-cost-isospo-coupling-circuitry-for-high-voltage-high-capacity-battery-systems.html> [Accessed: 2023/03/19]
- [3] *Application Notes for EV/LEV Contactors*, TE Connectivity, 2013. [Online]. Available: <https://www.flamecorp.com/PDF/TE-Connectivity/Kilovac/Application%20Notes%20for%20EV-LEC%20Contactors.pdf> [Accessed: 2023/03/19]
- [4] *LEV100H Extended Performance w/ Aux Contact Data Sheet*, TE Connectivity, 2016. [Online]. Available: https://www.te.com/commerce/DocumentDelivery/DDEController?Action=showdoc&DocId=Data+Sheet%7FSD-LEV100H%7FG%7Fpdf%7FEnglish%7FENG_DS_SD-LEV100H_G.pdf%7F1618408-2 [Accessed: 2023/03/19]
- [5] *ISOMETER® IR155-3203/IR155-3204. Isolationsüberwachungsgerät für ungeerdete DC-Antriebssysteme (IT-Systeme) in Elektrofahrzeugen.*, BENDER, 2021, Version V004. [Online]. Available: https://www.bender.de/fileadmin/content/Products/d/d/IR155-32xx-V004_D00115_D_XXDE.pdf [Accessed: 2022/09/23]
- [6] EEPOWER, "Resistor Sizes and Packages ." [Online]. Available: <https://eepower.com/resistor-guide/resistor-standards-and-codes/resistor-sizes-and-packages/> [Accessed: 2023/03/31]
- [7] *ITS4200S-ME-P. Smart High-Side NMOS-Power Switch*, Infineon, 2012. [Online]. Available: https://www.infineon.com/dgdl/Infineon-ITS4200S_ME_P_01092012S-DS-v01_00-en.pdf?fileId=db3a304339dcf4b1013a0140684a5741 [Accessed: 2023/03/26]
- [8] *SN74HCS08 Quadruple 2-Input AND Gates with Schmitt-Trigger Inputs*, Texas Instruments, 2021. [Online]. Available: <https://www.ti.com/lit/ds/symlink/sn74hcs08.pdf> [Accessed: 2023/03/26]
- [9] *Energy saving off-line high voltage converter*, STMicroelectronics, 2020. [Online]. Available: <https://www.st.com/resource/en/datasheet/viper01.pdf> [Accessed: 2023/04/02]
- [10] *STEVAL-ISA178V1 5 V/1 W 30 kHz buck demo with VIPer01*, STMicroelectronics, 2016. [Online]. Available: https://www.st.com/resource/en/application_note/an4858-stevalisa178v1-5-v1-w-30-khz-buck-demo-with-viper01-stmicroelectronics.pdf [Accessed: 2023/04/02]
- [11] *WE-PD HV SMT Power Inductor (High Voltage)*, Würth Elektronik eiSos GmbH & Co. KG, 2019. [Online]. Available: <https://www.we-online.com/components/products/datasheet/7687709332.pdf> [Accessed: 2023/04/02]
- [12] *Micropower, Low Voltage, Dual Comparator with 400mV Reference*, Analog Devices, 2021. [Online]. Available: <https://www.analog.com/media/en/technical-documentation/data-sheets/lt6700-6700hv.pdf> [Accessed: 2023/04/02]

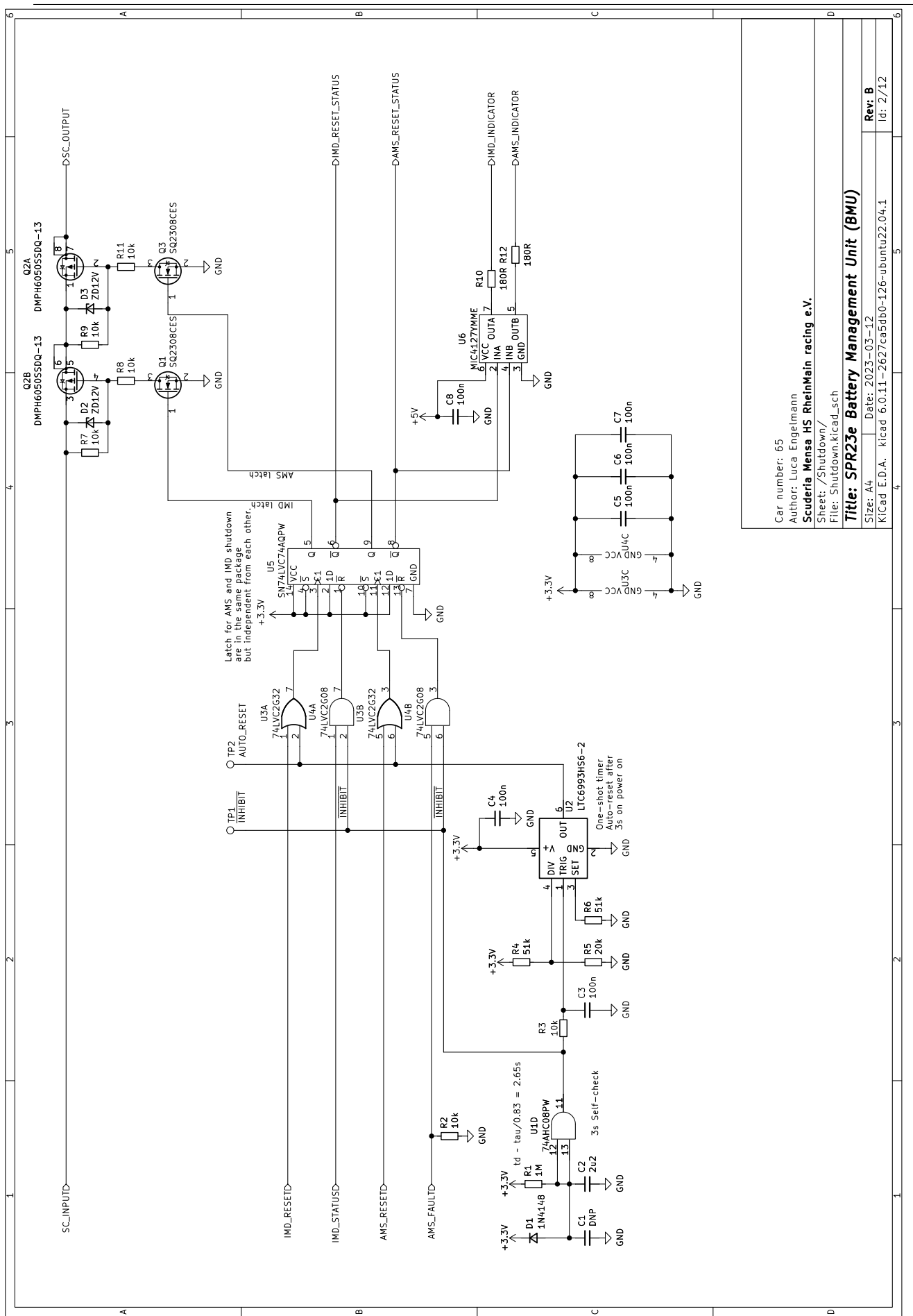


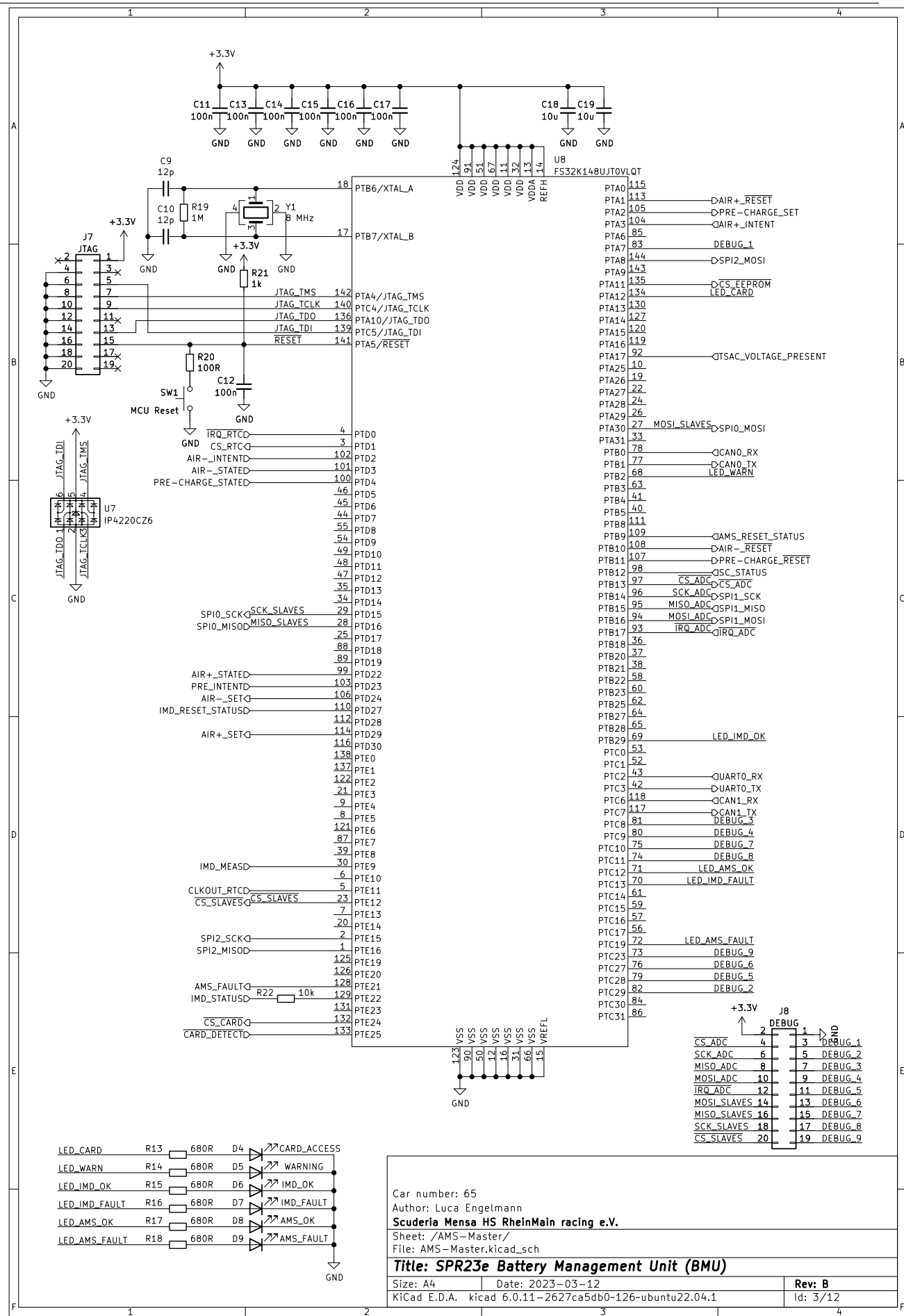
-
- [13] NXP, "S32K144-Q100 Evaluation Board for Automotive General Purpose." [Online]. Available: <https://www.nxp.com/design/development-boards/automotive-development-platforms/s32k-mcu-platforms/s32k144-q100-evaluation-board-for-automotive-general-purpose:S32K144EVB> [Accessed: 2023/03/26]

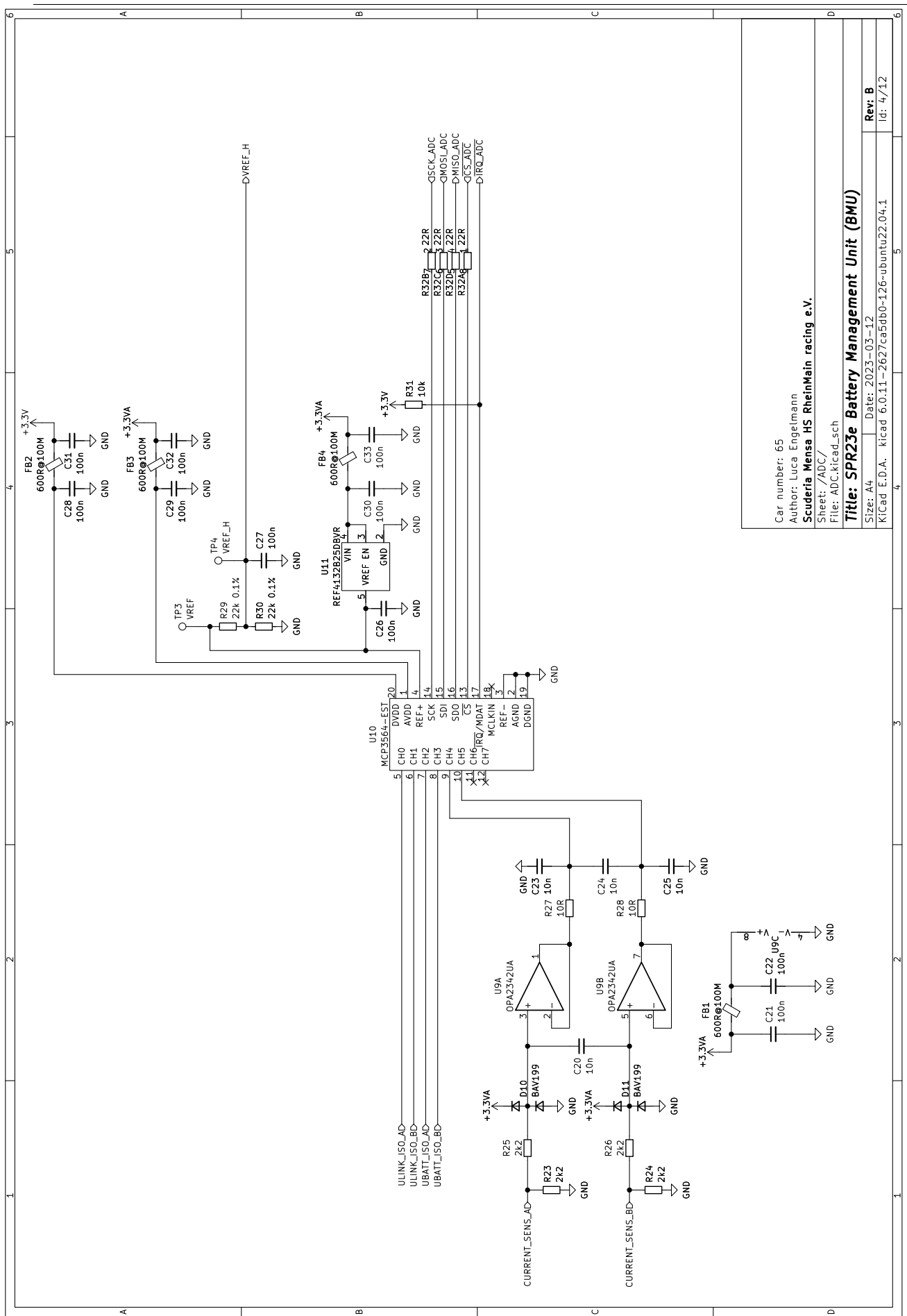


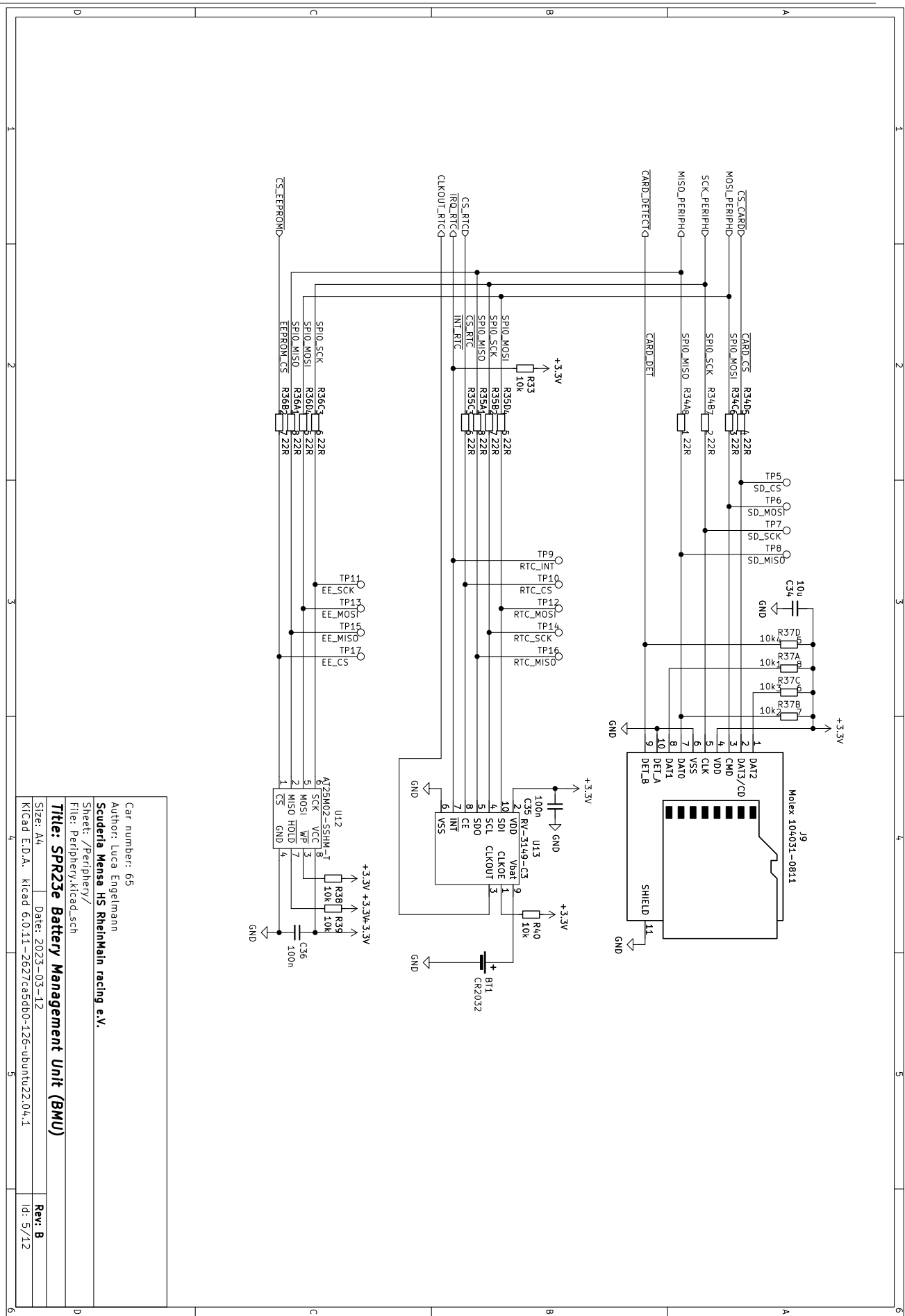
A. Schematics Revision A (Only for reference!)

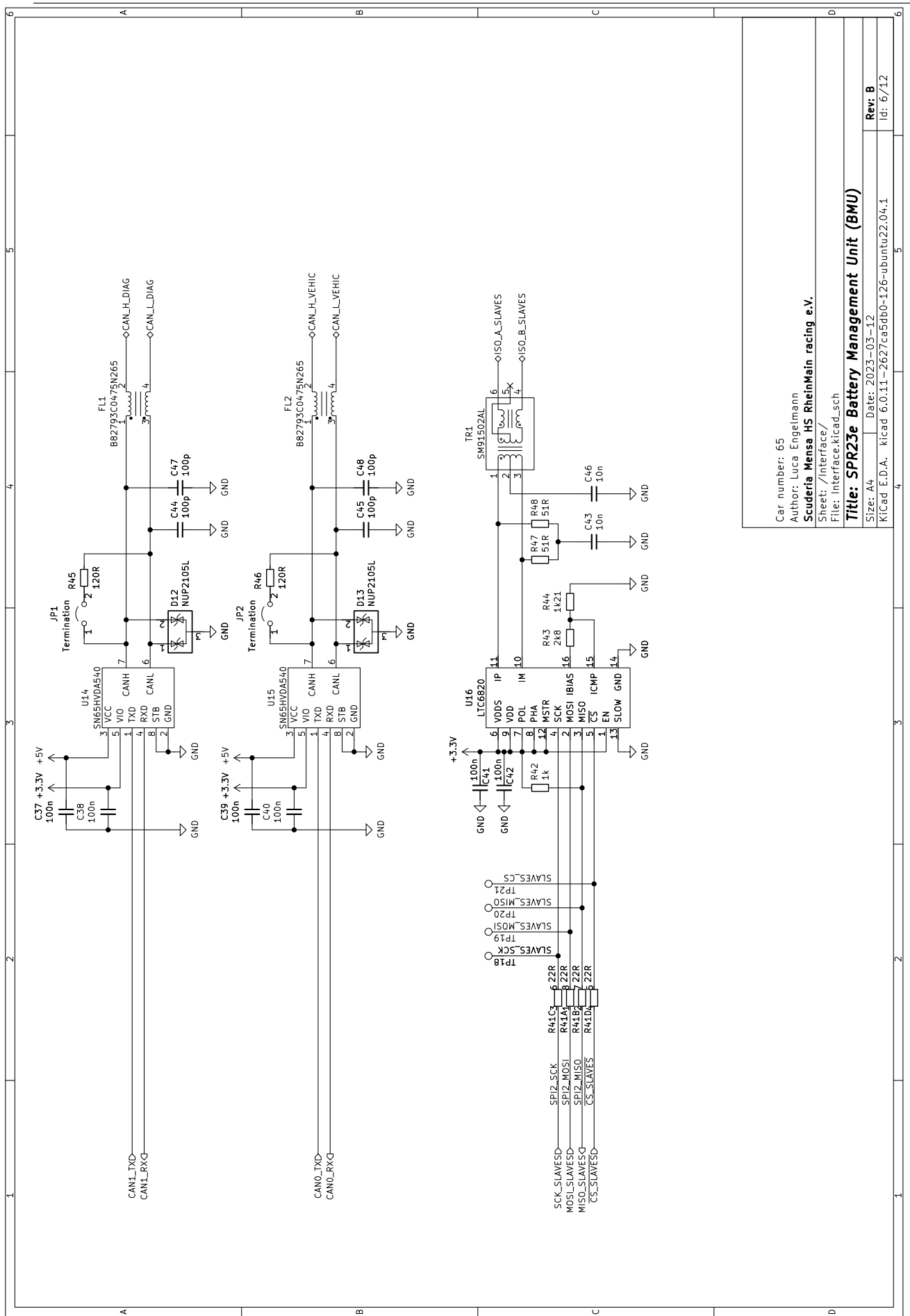


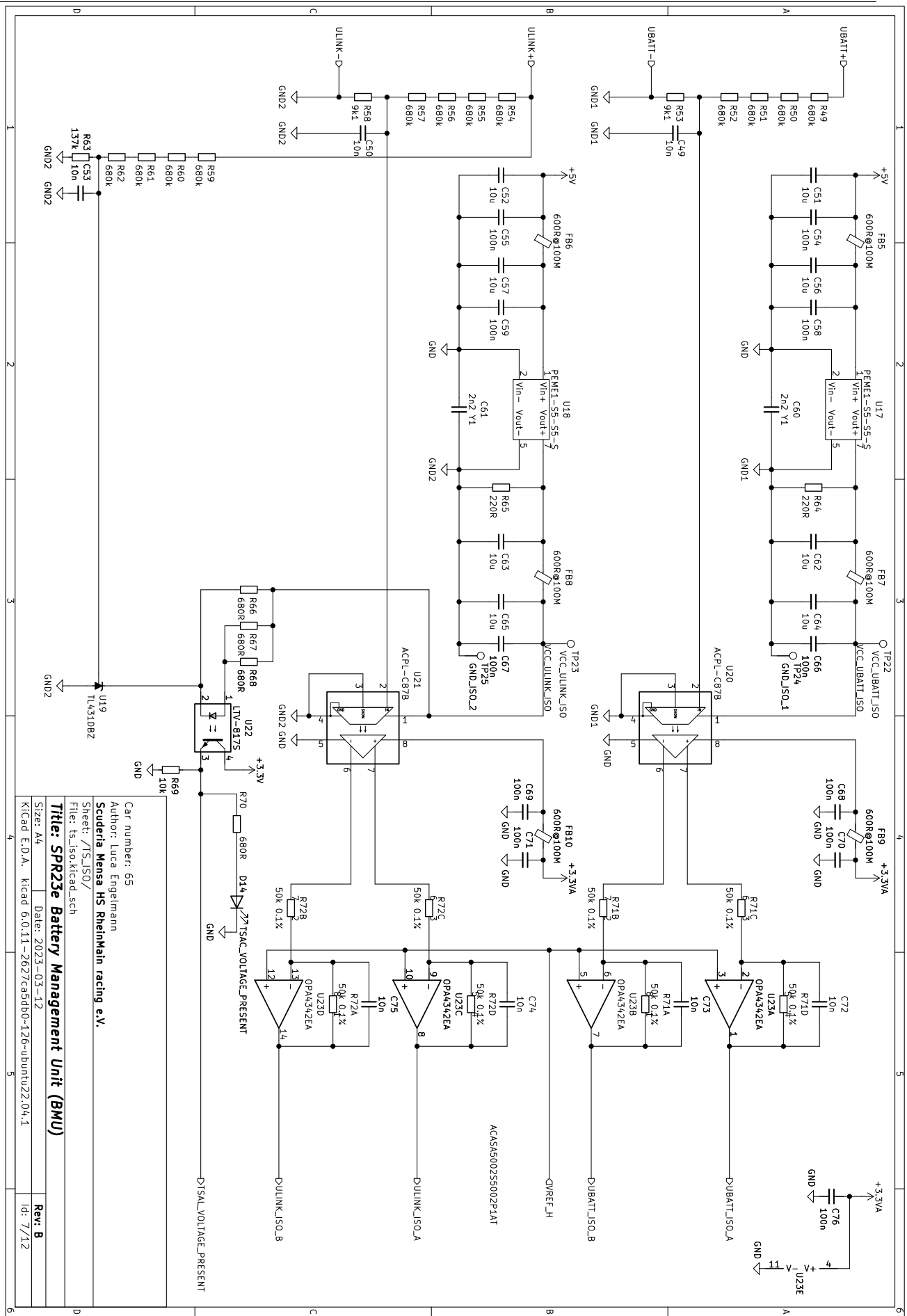


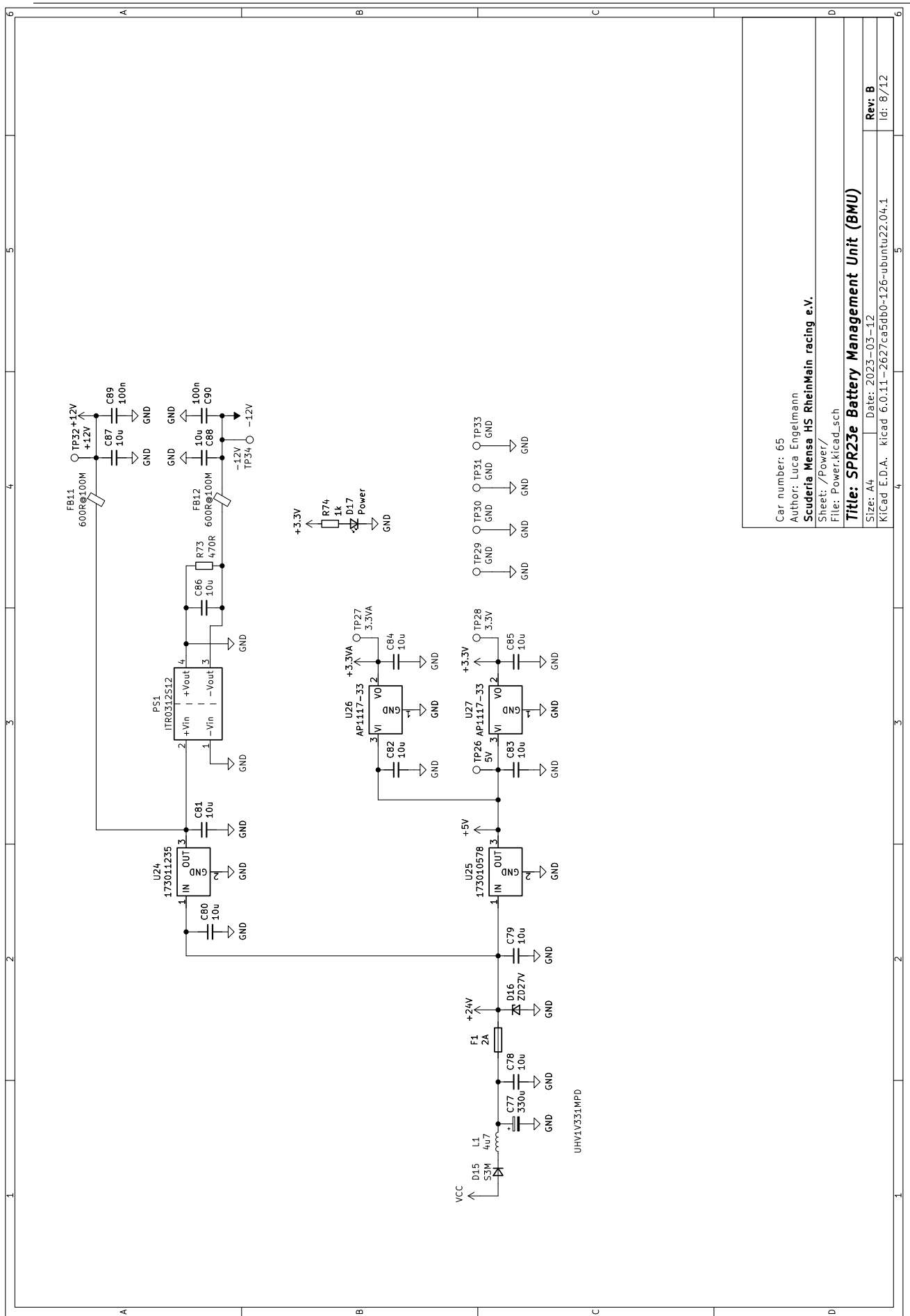


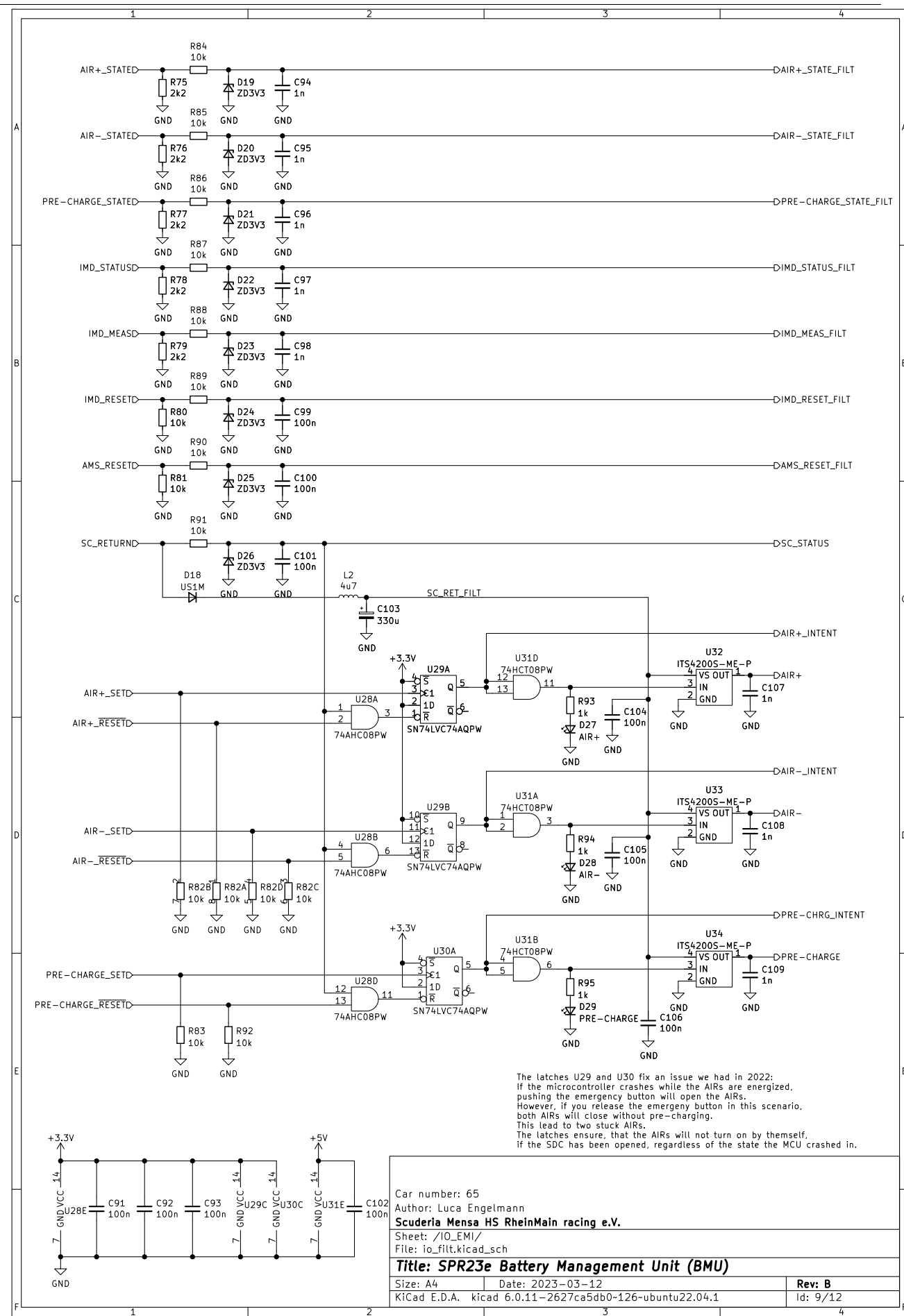


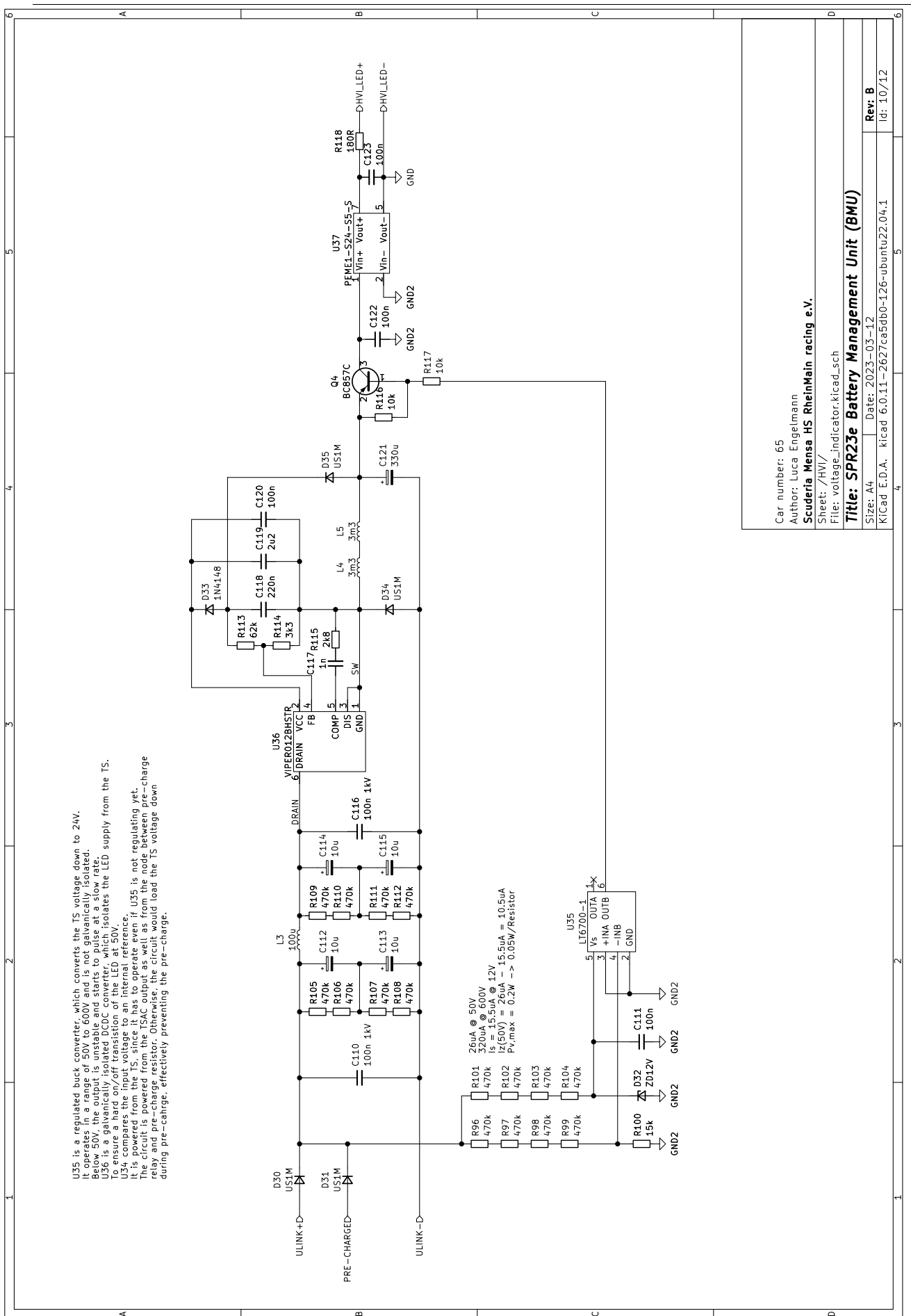








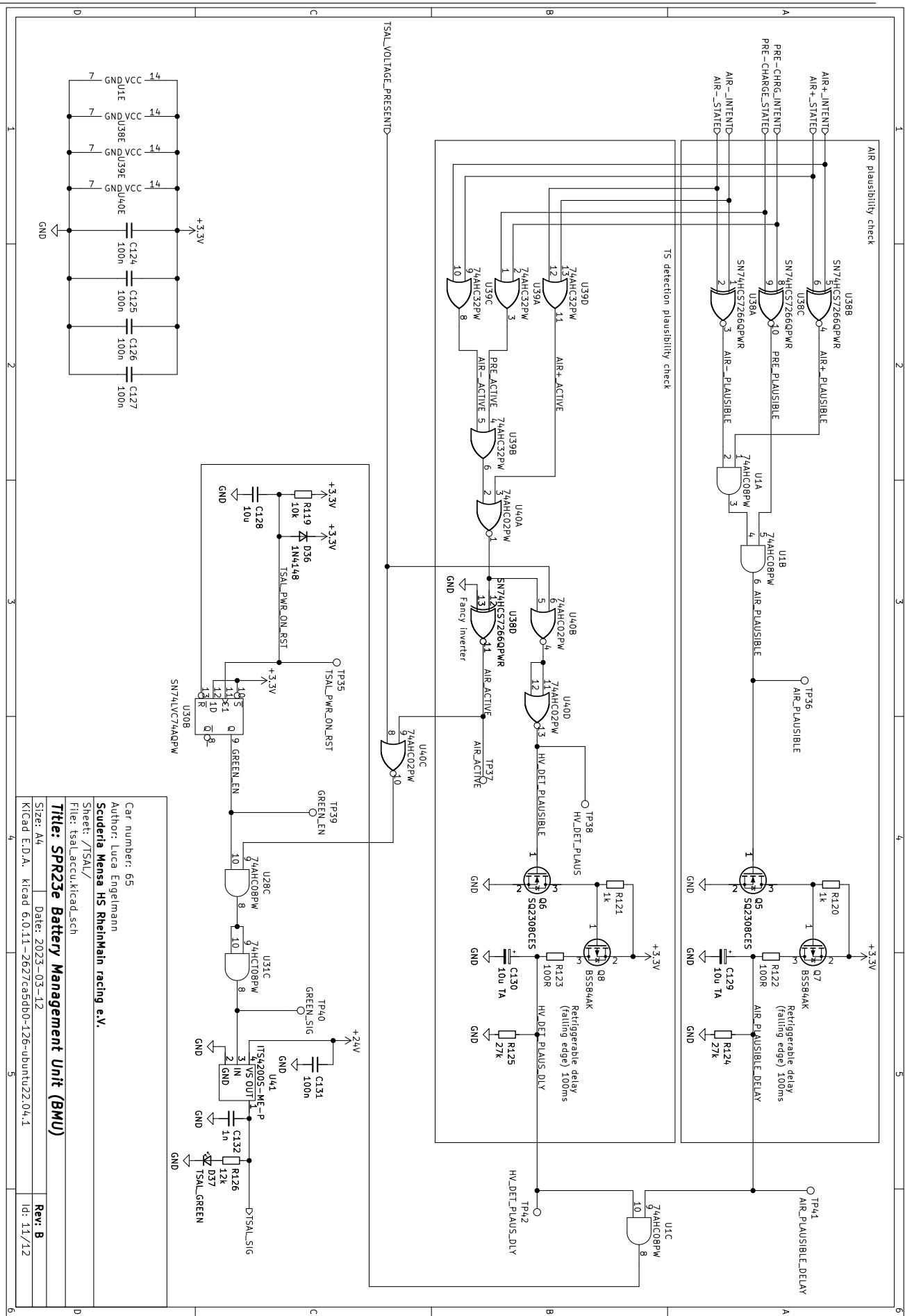


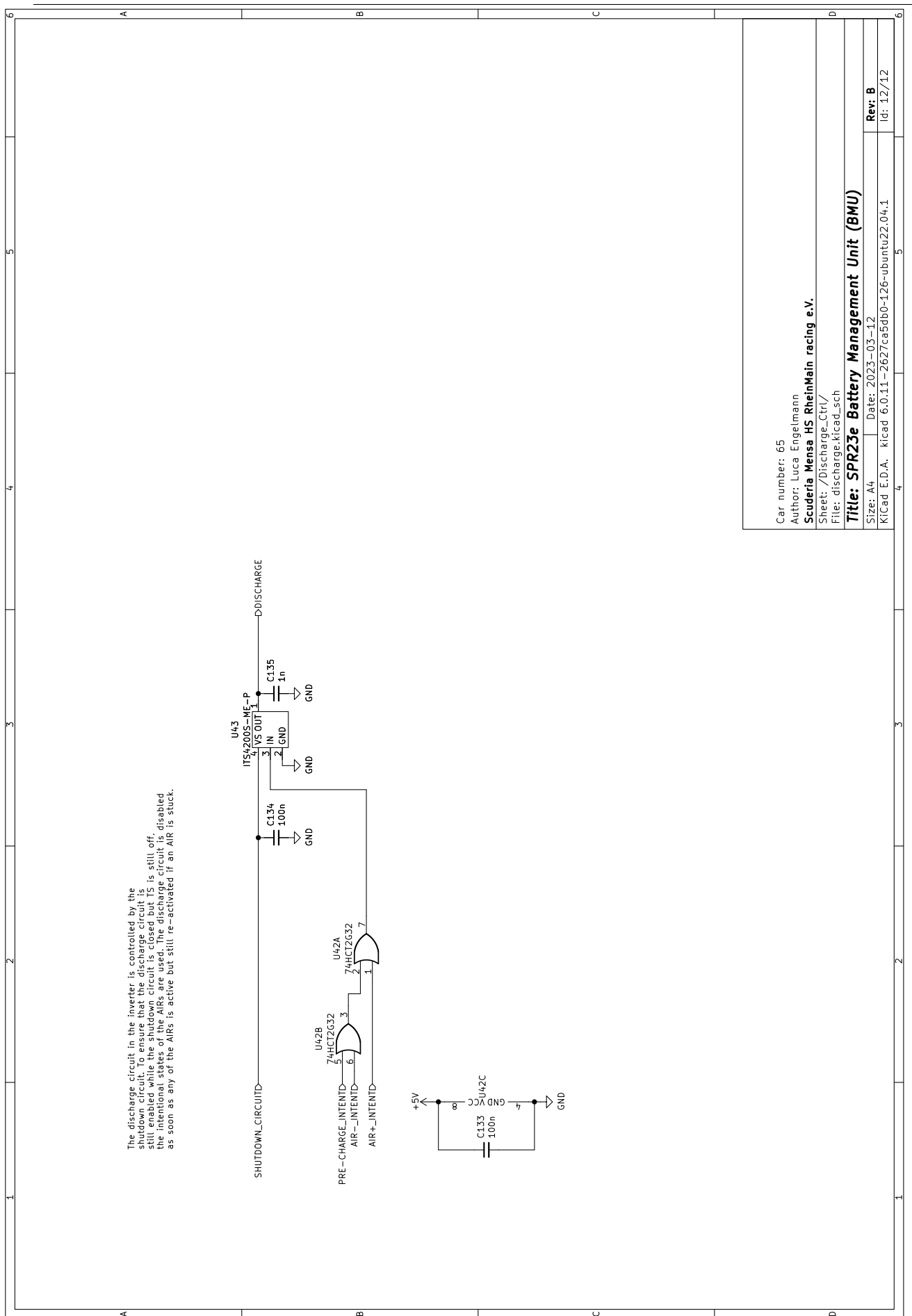


Car number: 65
Author: Luca Engelmann
Scuderia Mensa HS RheinMain racing e.V.

Sheet: /HVI/
File: voltage-indicator.kicad.sch

Title: SPR23e Battery Management Unit (BMU)		Rev: B
Size: A4	Date: 2023-03-12	
KICAD E.D.A. Kicad 6.0.11-2627ca5db0-126-ubuntu22.04.1	Id: 10/12	





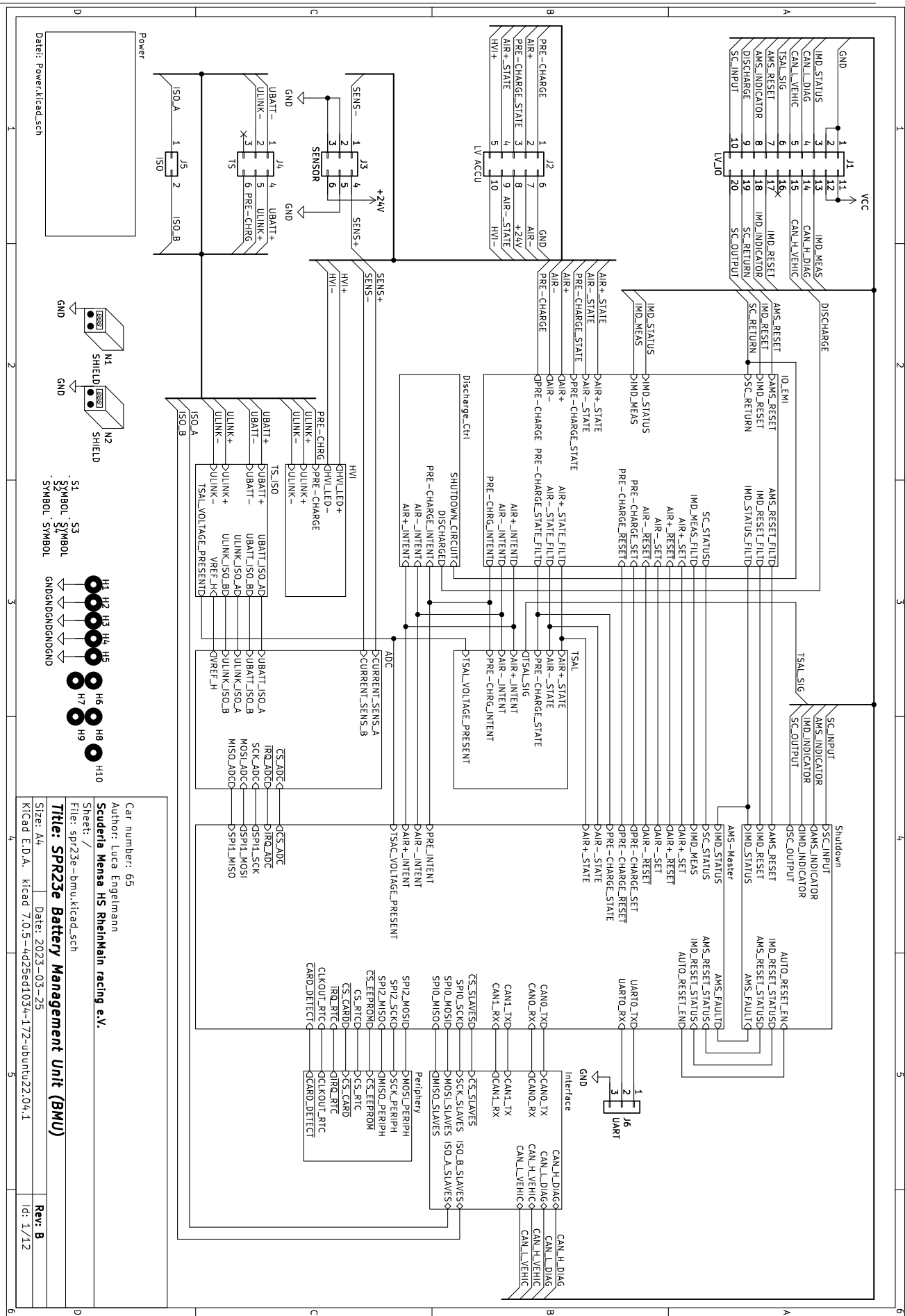


B. Changelog Revision B

- Corrected pinout of 74xx08
- Corrected pinout of 74xx2G08
- Corrected pinout of 74xx32
- Corrected pinout of 74xx2G32
- 74AHC08PW has no "real" Schmitt trigger inputs. Replaced by SN74HCS08.
- Removed ± 12 V power supplies from the BMU to clear out some space. It is only needed for the current sensor. Therefore it has been moved to the sensor PCB.
- Different comparator circuit for the voltage indicator for a sharp transition between on and off.
- Added minimum load for the isolated DCDC converters
- Increased the resistance value of the zener diode current limiting resistors at the inputs.
- Added test points for VREF, VREF_H and the outputs of the isolated DCDC converters.
- Increased the power-on-reset time for the TSAL latch
- Added ESD and overvoltage protection for the current sensor inputs
- Corrected the footprints of the electrolytic capacitors
- Corrected the footprints of the EMI suppression capacitors
- Corrected the control of the indicator LEDs. The LEDs must light up, if the power stage is disabled.
- Added pull-down resistor for the AMS fault signal
- Added a diode between SC_RET_FILT and SC_RETURN to decouple the high power signal from the low power signal.
- Typos corrected
- Changed reverse polarity protection diode for a higher current type
- Changed LED dropper resistors for equalized brightness
- Changed shutdown circuit auto-reset time to 3 s since IMD takes up to two seconds to power up.
- Only one power LED at the 3.3 V rail
- Reduced the delay time for the AIR plausibility to 100 ms to reduce BOM. 100 ms is sufficient.



C. Schematics Revision B



Date: Power.kicad_sch

Symbol: .SYMBOL

Symbol: .SYMBOL

Symbol: .SYMBOL

Symbol: .SYMBOL

Symbol: .SYMBOL

Car number: 65

Author: Luca Engelmann

Scuderia Mensa HS RheinMain racing e.V.

Sheet: /

File: sprz3e-bmu.kicad.sch

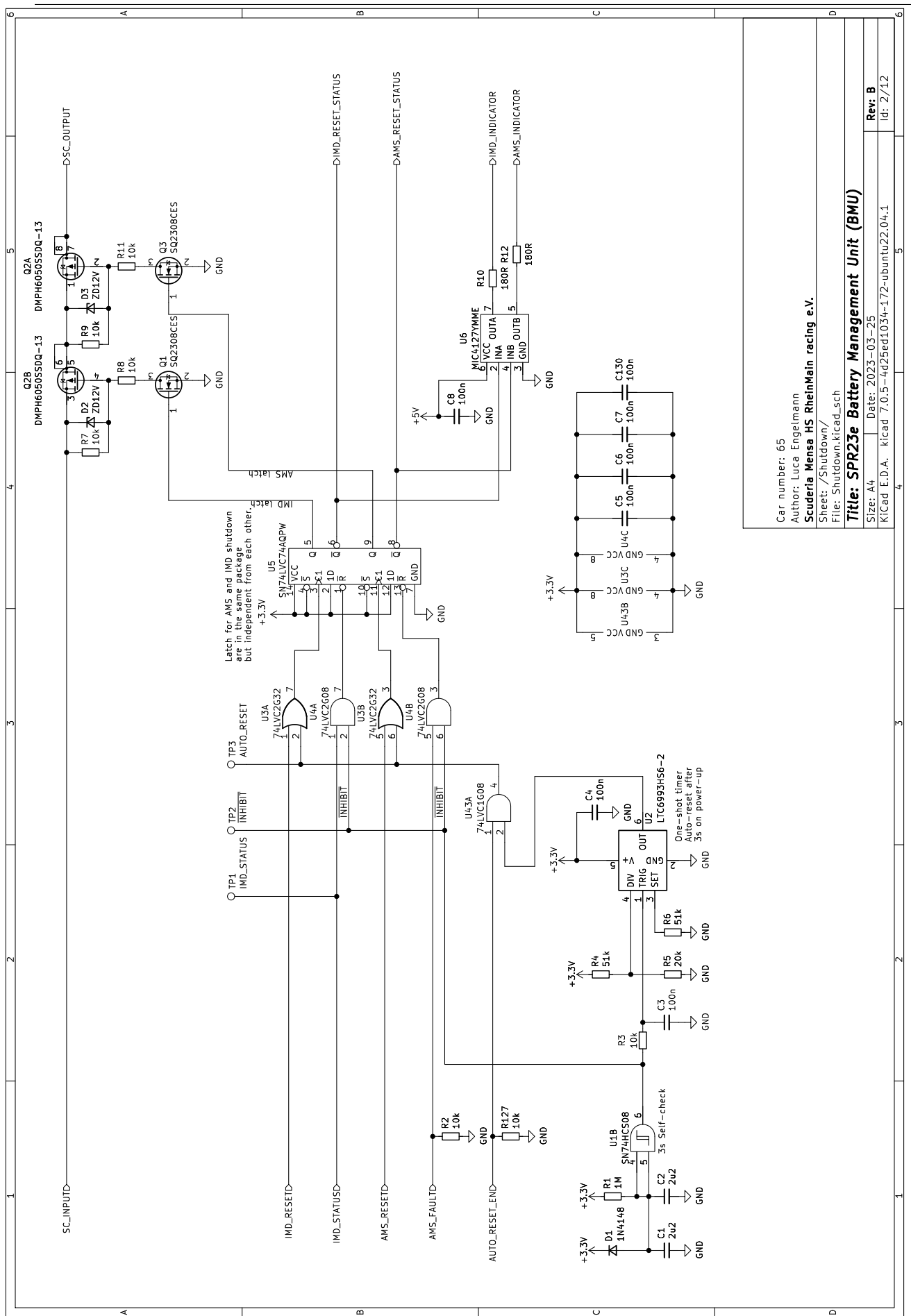
Size: A4

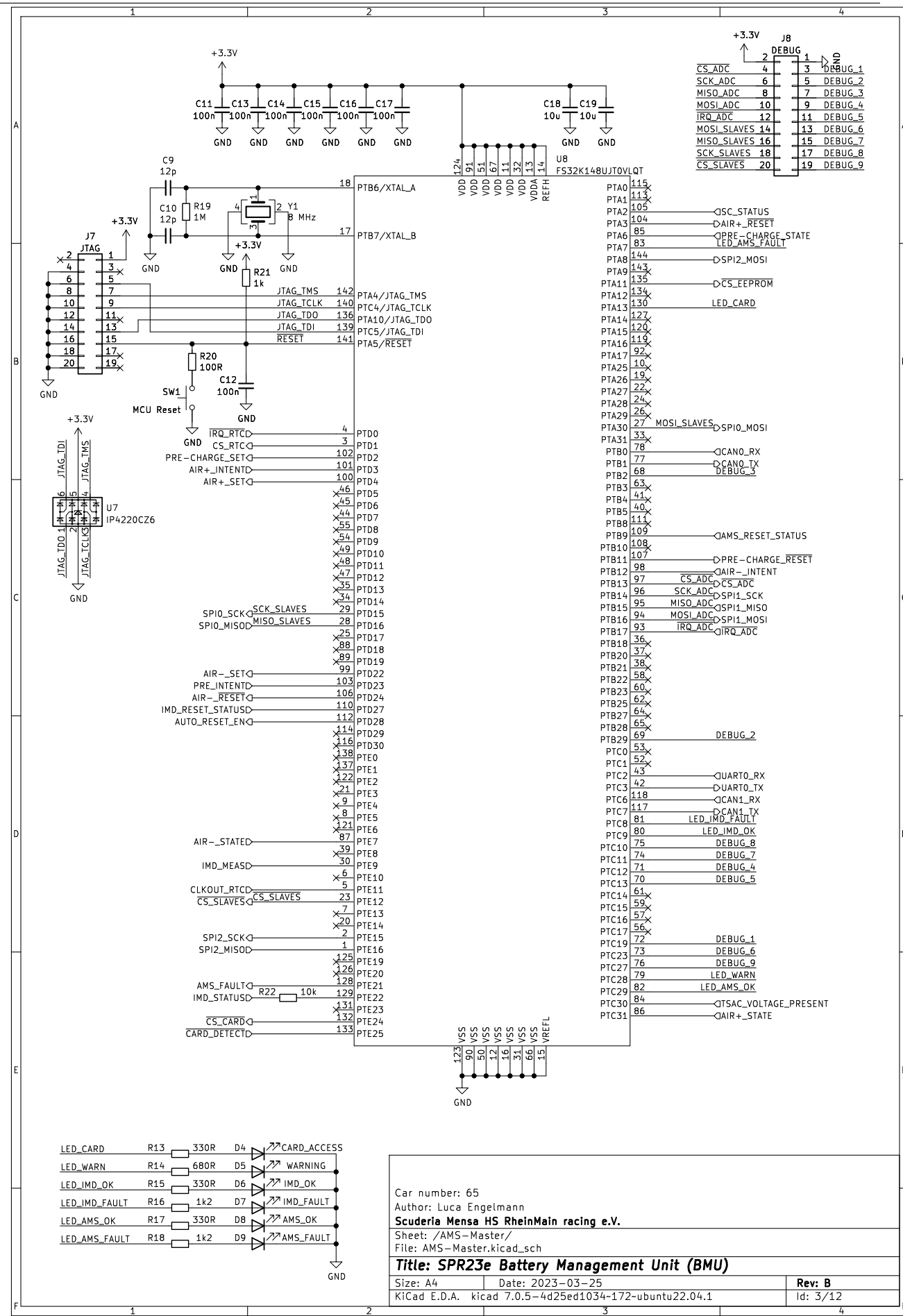
Date: 2023-03-25

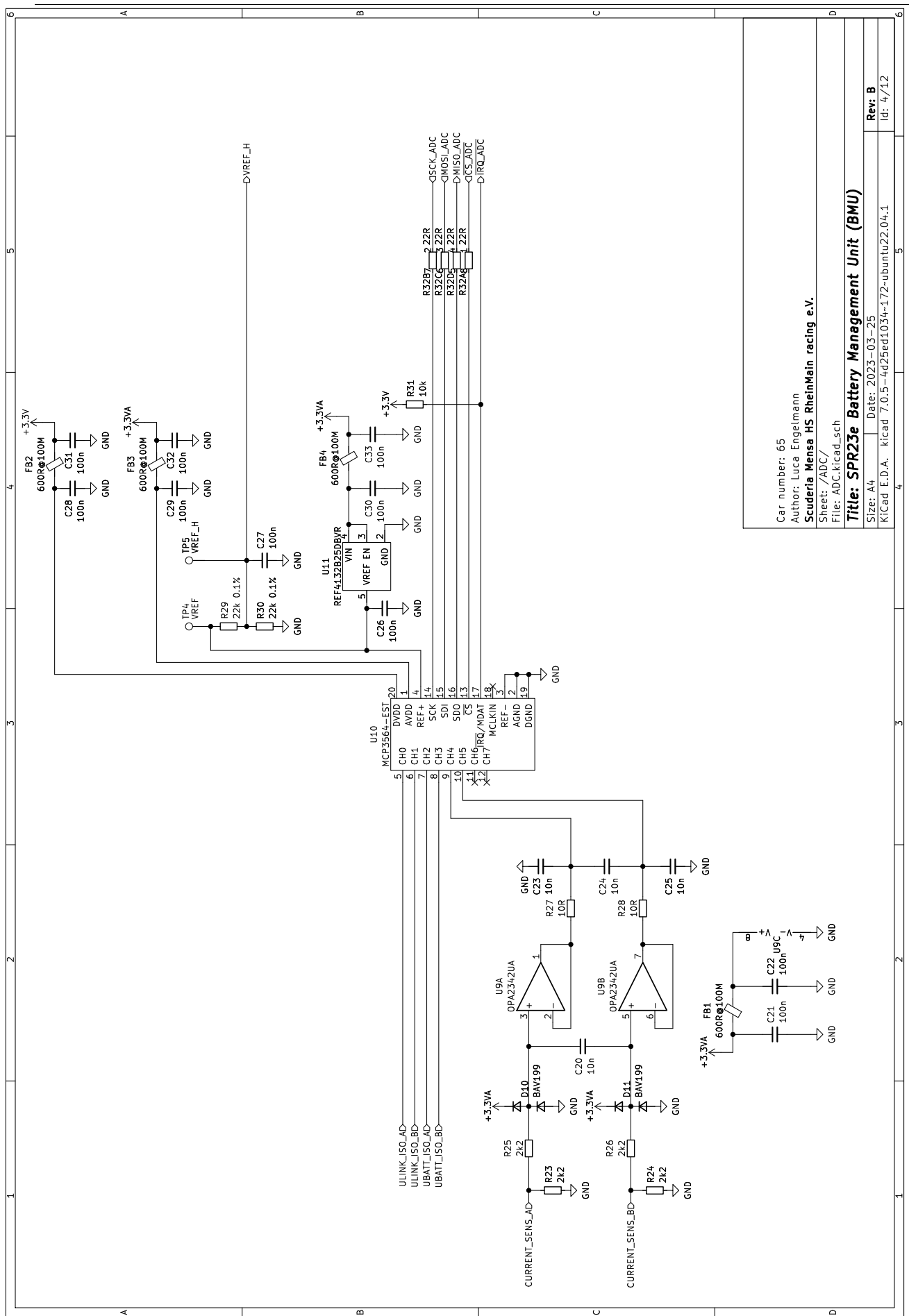
KICAD EDA

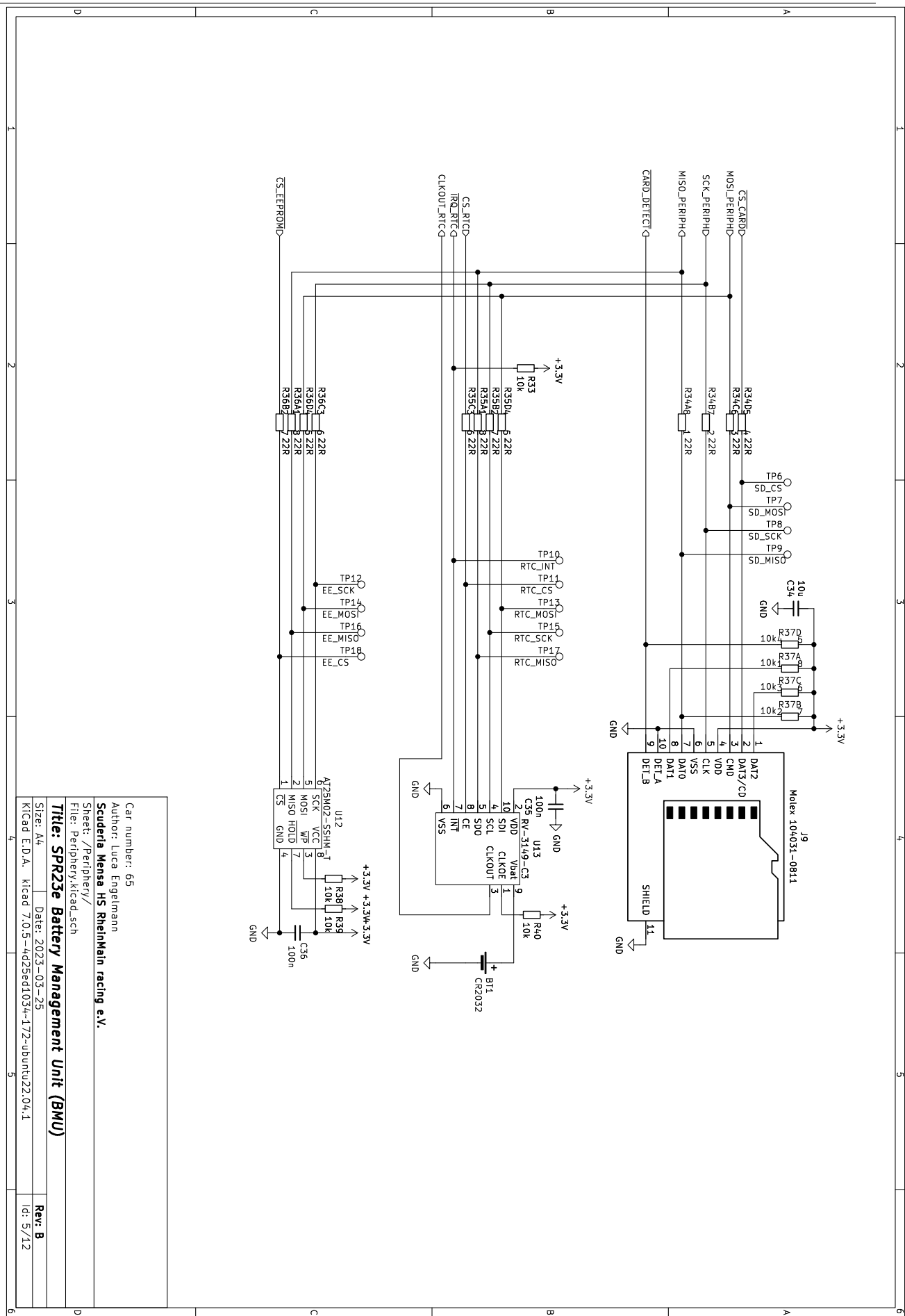
kicad 7.0.5 -4d25ed1034-172-ubuntu22.04.1

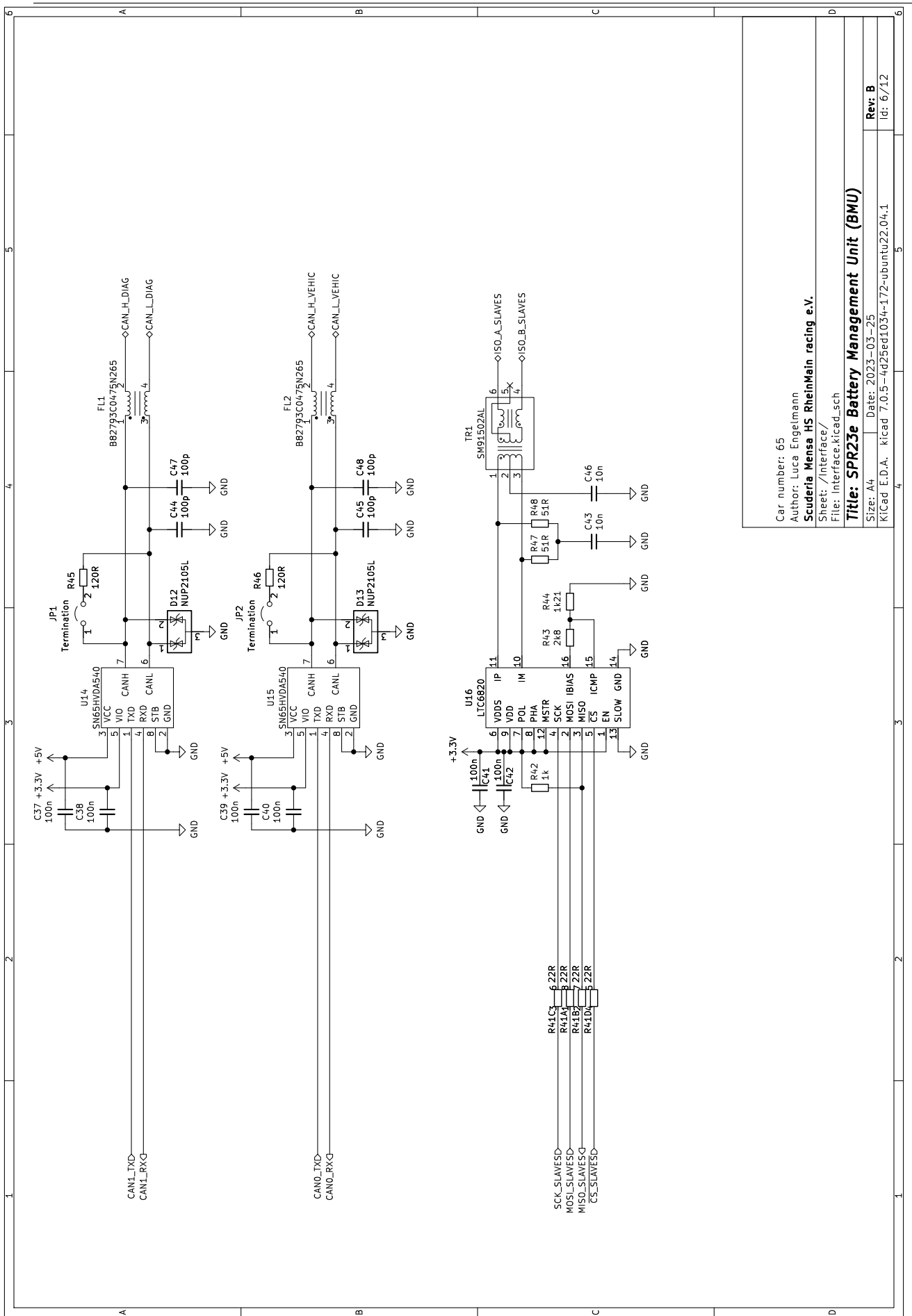
Id: 1/12

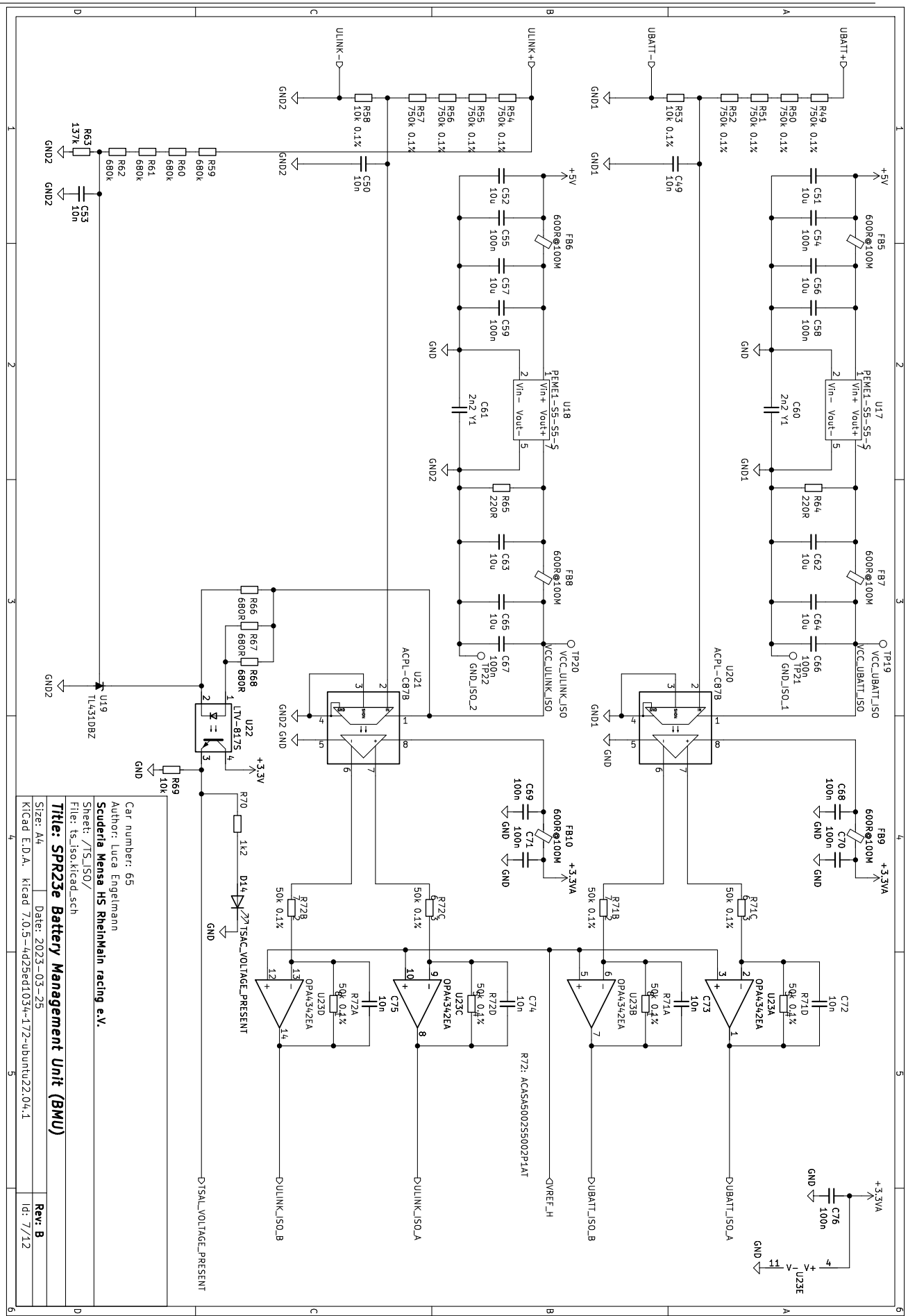


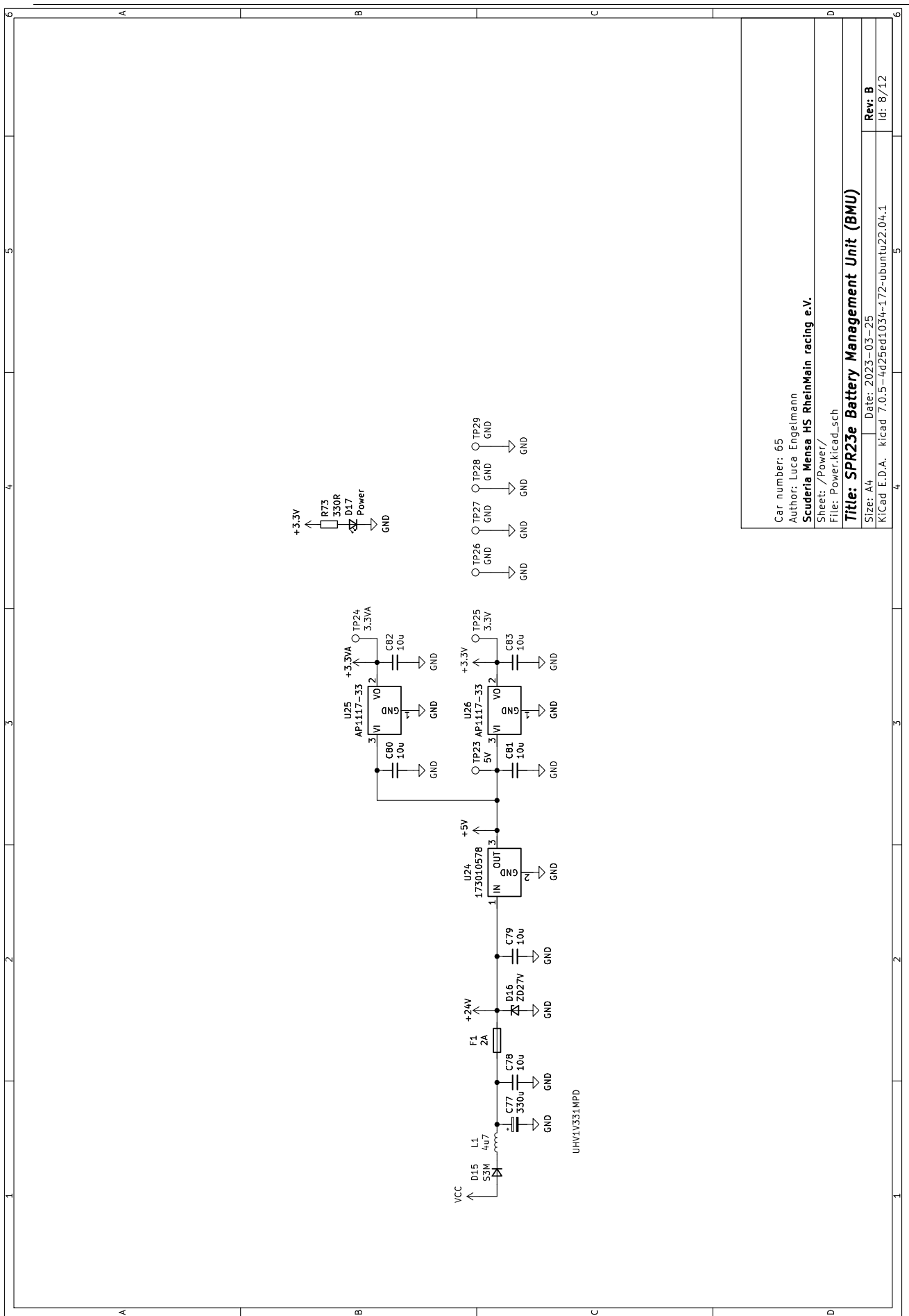












Car number: 65
Author: Luca Engelmann
Scuderia Mensa HS RheinMain racing e.V.

Sheet: /Power/
File: Power.kicad.sch

Title: SPR23e Battery Management Unit (BMU)

Rev: B
Size: A4 Date: 2023-03-25

Kicad 7.0.5-4d5ed1034-172-ubuntu22.04.1

Id: 8/12

5

4

3

2

1

C

B

A

6

